Since January 2020 Elsevier has created a COVID-19 resource centre with free information in English and Mandarin on the novel coronavirus COVID-19. The COVID-19 resource centre is hosted on Elsevier Connect, the company's public news and information website.

Bioorganic Chemistry 117 (2021) 105466

Contents lists available at ScienceDirect

Bioorganic Chemistry

journal homepage: www.elsevier.com/locate/bioorg

Synthesis of aspirin-curcumin mimic conjugates of potential antitumor and anti-SARS-CoV-2 properties

Aladdin M. Srour [a], Siva S. Panda [b], Ahmed Mostafa [c], Walid Fayad [d], May A. El-Manawaty [d], Ahmed A. F. Soliman [d], Yassmin Moatasim [c], Ahmed El Taweel [c], Mohamed F. Abdelhameed [e], Mohamed S. Bekheit [f], Mohamed A. Ali [c], Adel S. Girgis [f,*]

[a] Department of Therapeutic Chemistry, National Research Centre, Dokki, Giza 12622, Egypt
[b] Department of Chemistry & Physics, Augusta University, Augusta, GA 30912, US
[c] Center of Scientific Excellence for Influenza Viruses, National Research Centre, Giza 12622, Egypt
[d] Drug Bioassay-Cell Culture Laboratory, Pharmacognosy Department, National Research Centre, Dokki, Giza 12622, Egypt
[e] Pharmacology Department, National Research Centre, Dokki, Giza 12622, Egypt
[f] Department of Pesticide Chemistry, National Research Centre, Dokki, Giza 12622, Egypt

ARTICLE INFO

Keywords:
4-Piperidone
Aspirin
Antitumor
VEGFR-2
EGFR
COX-1/2
SARS-CoV-2

ABSTRACT

Series of piperidone-salicylate conjugates were synthesized through the reaction of 3*E*,5*E*-bis(arylidene)-4-piperidones with the appropriate acid chloride of acetylsalicylate in the presence of triethylamine. All the synthesized conjugates reveal antiproliferative properties against A431 (squamous skin) cancer cell line with potency higher than that of 5-fluorouracil. Many of the synthesized agents also exhibit promising anti-proliferative properties against HCT116 (colon) cancer cell line, of which **5o** and **5c** are the most effective with 12.9, 9.8 folds potency compared with Sunitinib. Promising activity is also shown against MCF7 (breast) cancer cell line with 1.19, 1.12 folds relative to 5-fluorouracil. PI-flow cytometry of compound **5c** supports the arrest of cell cycle at G1-phase. However, compound **5o** and Sunitinib arrest the cell cycle at S-phase. The synthesized conjugates can be considered as multi-targeted tyrosine kinase inhibitors due to the promising properties against VEGFR-2 and EGFR in MCF7 and HCT116. CDOCKER studies support the EGFR inhibitory properties. Compounds **5p** and **5i** possessing thienylidene heterocycle are anti-SARS-CoV-2 with high therapeutic indices. Many of the synthesized agents show enhanced COX-1/2 properties than aspirin with better selectivity index towards COX-2 relative to COX-1. The possible applicability of the potent candidates discovered as antitumor and anti-SARS-CoV-2 is supported by the safe profile against normal (non-cancer, RPE1 and VERO-E6) cells.

1. Introduction

Natural products are still the main resources of human needs. Many therapeutics were designed due to inspiration of the biologically active natural compounds [1]. Curcumin is a natural compound (isolated from *Curcuma longa*) [2] gained interest due to its broad range biological properties as anti-inflammatory [3], anticancer [4-6] and antimicrobial [7]. Although its safety profile, the clinical applications are hindered due to its bioavailability (low aqueous or plasma solubility and stability at physiological pH) [8,9]. This is why curcumin mimics were alternatively considered by many researchers. It is believed that the active methylene connecting the β-diketonic moieties plays a crucial role in curcumin stability [10,11]. The diene connected through a carbonyl group forming a five-carbon system seems an acceptable approach for developing a biologically enhanced scaffold [12-14]. 3,5-Diylidene-4-piperidones are curcumin mimics with broad promising biological properties of which antitumor against diverse cancer cell lines [15-18] and anti-inflammatory [19]. The present study deals with synthesis of 3,5-bis(arylidene)-4-piperidones as curcumin mimics conjugated with acetylsalicylic acid (aspirin) (Fig. 1).

Since the discovery of aspirin by Felix Hoffman of Bayer industry (1897), it became one of the most usable low-cost NSAIDs (non-steroidal anti-inflammatory drugs) worldwide, accessible as an analgesic and anti-inflammatory therapeutic [20,21]. It has been also reported that, daily low dose aspirin reduces heart attack risks [22]. Gastrointestinal ulcer is the most serious drawback of aspirin similar to many other

* Corresponding author.
E-mail address: girgisas10@yahoo.com (A.S. Girgis).

https://doi.org/10.1016/j.bioorg.2021.105466
Received 6 October 2021; Accepted 31 October 2021
Available online 4 November 2021

NSAIDs [23]. This is attributable to the irritation formed due to direct contact of the NSAID carboxylic group with the tissue(s) producing prostaglandin [24]. Enteric-coated aspirin was considered to overcome the gastrointestinal ulceration side effects but the reduced efficacy especially in chronic administration and coronary heart disease hindered the applicability [25,26]. Many reports mentioned that aspirin can reduce the risk of cancer [27-33] and inhibit NFκβ signal which may assist in cancer growth and metastasis [34,35]. This is why many researchers adopted investigation of aspirin based-analogues as potential antitumor candidates [36-39]. Others considered conjugation of aspirin with antitumor chemotherapeutics [40] because inflammation initiated by cancer may lead to metastasis [41]. Furthermore, the reported antitumor properties of salicylamide-containing compounds [42-44] prompted the current study due to the targeted salicylamide derivative formed through conjugation of the carboxylic group of aspirin with the nitrogen atom of piperidinyl heterocycle. Recent reports describing the pathophysiological role of COX-1/2 inhibitors in cancer disease and the discovered COX-2 inhibitors as antitumor also supported the rational of the current study [45,46].

Although the continuous advances/efforts in diagnosis and treatment in cancer research, it is still one of the most serious challenges for human health. It is the second cause of death globally after cardiovascular diseases [47]. It is expected the number of deaths will exceed those of any other disease and be the first cause of human mortality within few years [48]. Needs for more therapeutic approaches especially, new chemotherapies with higher efficacies and fewer drawbacks are still in demand. The designed agents of the current study will be considered for antitumor evaluation against HCT116 (colon), MCF7 (breast) and A431 (squamous skin) cancer cell lines. Selection of the mentioned cancer cell lines among many other types are due to promising properties reported by the piperidone-containing compounds [15,16,49]. Colorectal (including colon and rectum) cancer is the third leading cause of death globally among all cancer types. The five year survival due to colon cancer is still high (30%) due to the recurrence and metastasis [50]. Many factors are overlapped in colon cancer including heredity, colon polyps, and ulcerative colitis. Colon cancer usually arises from colon polyps [49]. Surgery is the most accepted optional approach for localized colon cancer. However, chemotherapy is the most successful for metastasis [51]. Breast cancer is the fifth cause of human cancer death and the second for women [52,53]. Surgery, chemotherapy, radiotherapy, immunotherapy and hormone therapy, are still the main options for breast cancer [53,54]. Skin cancer incidence and mortality are increased in the last few years [55]. This is attributed to many factors including exposure to sunlight (ultraviolet radiation) [56] and genetic predisposition [57]. Skin cancers are of two main types, melanoma and non-melanoma (basal and squamous) cell carcinoma. Although the non-melanoma cancers are the more prevalent, melanoma skin cancer is more aggressive with a higher number of deaths [58].

By the end of 2019 a new disease was started in Wuhan, China [59] by an unknown infectious virus "SARS-CoV-2 (respiratory syndrome coronavirus 2)", which was identified as single stranded RNA virus coronavirus (family *Betacoronavirus*) [60]. It is speedy spread to all continents of the world (about 230.4 million affected patients with 4.7 million deaths [61]) exhibiting great challenge to the global health system due to lack of powerful clinical treatments. This is why WHO (World Health Organization) declared a pandemic COVID-19 (corona virus disease 2019) on March 11, 2020 [62]. Although previous coronaviral diseases were declared (SARS-CoV, Foshan, China, Nov. 2002 and MERS-CoV "Middle East Respiratory Syndrome", Jeddah, Saudi Arabia, June 2012) the current pandemic seems more aggressive due to the wide spreading and great number of deaths [63]. The scientific society with the pharmaceutical companies did their best for developing vaccine(s) that may control the viral prophylactic action and identifying/developing therapeutic agent(s) for infected patients. For optimizing an effective medication computational technique or drug reproposing were utilized to accelerate the identification of the urgent needs [59,64,65]. Many drugs were re-proposed/adopted for COVID-19 of which Lopinavir/Ritonavir, Chloroquine, Hydroxychloroquine, Arbidol, Remdesivir and Favipiravir (Fig. 2) but none of them seems of high efficacy especially for advanced infection [60,66-68]. This is why new effective agents are still in demand. Due to the reports mentioned for the anti-SARS-CoV-2 properties of diverse antitumor active agents [69-71], the targeted conjugates within the current study will be intended for anti-SARS-CoV-2 properties investigation. The successful clinical reports for treating the colon cancer patients with antiviral drugs alone or with antitumor drugs [72] also add good support for the aim of the present study directed towards optimizing new hits of dual functions as antitumor and anti-SARS-CoV-2 with safety properties against normal cells. Recent reports describing aspirin as anti-SARS-CoV-2 with mild properties and safe applicability also prompted the current study [73].

2. Results and discussion

2.1. Chemistry

The acid chlorides **3a,b** [74,75] were obtained from the corresponding acetylsalicylic acids **2a,b** [76] by the reported procedure [oxalyl chloride in dichloromethane containing a catalytic amount of *N,—N*—dimethylformamide (DMF)]. Reaction of the 3*E*, 5*E*-bis(arylidene)-4-piperidones **4a–i** [15,16,19,77,78] with the appropriate **3a,b** in DMF in presence of sufficient amount of triethylamine in an ice-cold water bath afforded the targeted conjugates **5a–p** in acceptable yields (60–88 %) (Scheme 1). IR spectrum of **5a** (an example of the targeted family) reveals the piperidinyl ketonic and salicylate amidic carbonyls at ν = 1767, 1643 cm^{-1}, respectively. ^1H NMR spectrum of **5a** shows the piperidinyl methylene protons as singlet signals at δ_H = 4.58, 5.01 and the salicylate singlet acetyl protons at δ_H = 2.14. However, the exocyclic olefinic methine protons are hidden under the aromatic protons. ^{13}C NMR spectrum of **5a** exhibits the piperidinyl methylene carbons at δ_C = 42.6, 47.2 and the acetyl carbon at δ_C = 20.4. The piperinyl carbonyl carbon is viewed at δ_C = 185.7 and the salicylate carbonyls at δ_C = 165.6, 168.4 (Supplementary Figs. S1-S48).

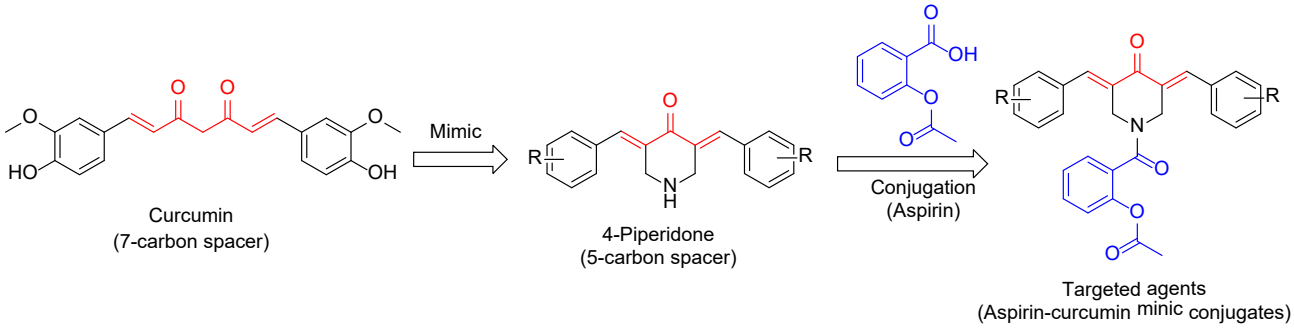

Fig. 1. Design of the targeted aspirin-piperidone conjugates.

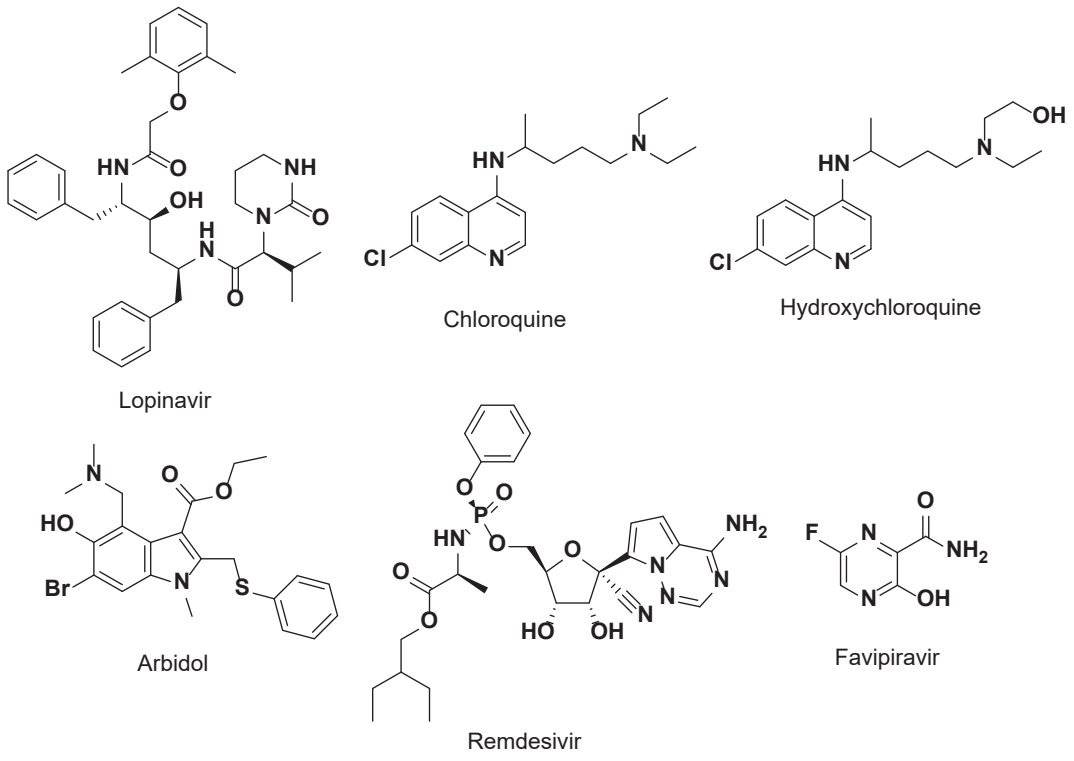

Fig. 2. Proposed drugs for COVID-19.

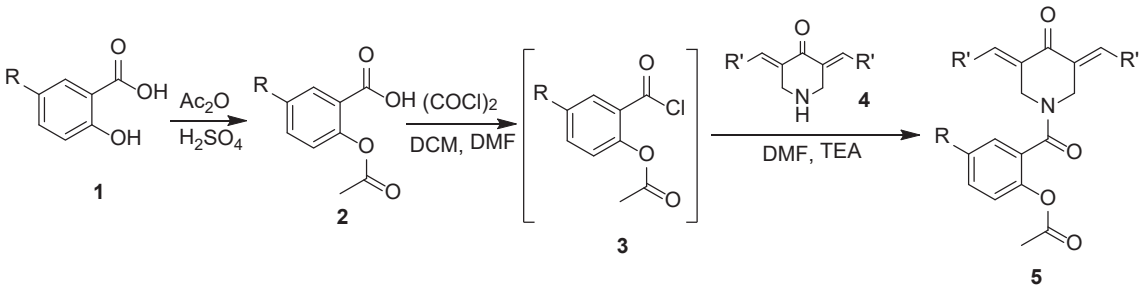

1a, **2a**, **3a**; R = H
1b, **2b**, **3b**; R = Cl

4a; R = Ph
4b; R = 4-FC_6H_4
4c; R = 4-ClC_6H_4
4d; R = 4-BrC_6H_4
4e; R = 4-$H_3CC_6H_4$
4f; R = 4-$H_3COC_6H_4$
4g; R = 3,4-$(H_3CO)_2C_6H_3$
4h; R = 3,4,5-$(H_3CO)_3C_6H_2$
4i; R = 2-thienyl

5a; R = H, R' = Ph (72%)
5b; R = H, R' = 4-FC_6H_4 (68%)
5c; R = H, R' = 4-ClC_6H_4 (69%)
5d; R = H, R' = 4-BrC_6H_4 (61%)
5e; R = H, R' = 4-$H_3CC_6H_4$ (67%)
5f; R = H, R' = 4-$H_3COC_6H_4$ (81%)
5g; R = H, R' = 3,4-$(H_3CO)_2C_6H_3$ (71%)
5h; R = H, R' = 3,4,5-$(H_3CO)_3C_6H_2$ (73%)
5i; R = H, R' = 2-thienyl (76%)
5j; R = Cl, R' = Ph (67%)
5k; R = Cl, R' = 4-ClC_6H_4 (88%)
5l; R = Cl, R' = 4-BrC_6H_4 (84%)
5m; R = Cl, R' = 4-$H_3COC_6H_4$ (87%)
5n; R = Cl, R' = 3,4-$(H_3CO)_2C_6H_3$ (61%)
5o; R = Cl, R' = 3,4,5-$(H_3CO)_3C_6H_2$ (60%)
5p; R = Cl, R' = 2-thienyl (75%)

Scheme 1. Synthetic route towards the targeted conjugates **5a–p**.

2.2. Biological studies

2.2.1. Antiproliferative properties

The standard MTT bioassay technique was considered for anti-proliferation properties determination of the synthesized agents **5a–p** [79]. Table 1 displays the IC_{50} (concentration capable for 50% growth inhibition of the tested cell line) of the synthesized agents **5a–p** and reference standards (5-fluorouracil and sunitinib) which are clinically approved drugs against the considered cancer cell lines (Supplementary Figs. S49-S52). FDA approved 5-fluorouracil for treatment colon, breast and skin cancers [80,81]. Sunitinib was approved for treatment of gastrointestinal, renal and pancreatic cancers [82,83].

Table 1
Antiproliferative properties of the synthesized agents, curcumin, 5-fluorouracil and Sunitinib.

Entry	Compd.	$IC_{50} \pm SE$, μM (SI)[a]			
		A431	MCF7	HCT116	RPE1
1	**5a**	4.486 ± 0.41 (2.4)	4.736 ± 0.38 (2.25)	4.722 ± 0.42 (2.25)	10.64 ± 1.04
2	**5b**	2.125 ± 0.19 (3.9)	5.764 ± 0.47 (1.44)	5.097 ± 0.51 (1.63)	8.30 ± 0.71
3	**5c**	1.208 ± 0.11 (7.3)	2.806 ± 0.26 (3.15)	0.986 ± 0.08 (8.96)	8.83 ± 0.68
4	**5d**	0.986 ± 0.08 (9.8)	4.583 ± 0.39 (2.11)	3.597 ± 0.29 (2.69)	9.68 ± 0.57
5	**5e**	0.639 ± 0.07 (15.5)	6.000 ± 0.50 (1.65)	2.556 ± 0.18 (3.87)	9.89 ± 0.75
6	**5f**	6.042 ± 0.62 (1.6)	5.375 ± 0.51 (1.84)	6.083 ± 0.49 (1.63)	9.89 ± 0.66
7	**5 g**	0.973 ± 0.07 (10.6)	4.972 ± 0.42 (2.08)	2.389 ± 0.21 (4.32)	10.32 ± 1.10
8	**5 h**	0.472 ± 0.02 (18.3)	3.986 ± 0.36 (2.16)	1.333 ± 0.09 (6.47)	8.62 ± 0.72
9	**5i**	2.153 ± 0.15 (8.8)	5.583 ± 0.52 (3.41)	9.255 ± 0.61 (2.06)	19.04 ± 0.99
10	**5j**	2.514 ± 0.18 (3.7)	4.500 ± 0.39 (2.06)	2.625 ± 0.19 (3.53)	9.26 ± 0.75
11	**5 k**	0.417 ± 0.03 (18.6)	4.069 ± 0.33 (1.91)	1.972 ± 0.17 (3.94)	7.77 ± 0.56
12	**5 l**	0.667 ± 0.07 (10.8)	4.153 ± 0.37 (1.74)	1.153 ± 0.13 (6.27)	7.23 ± 0.49
13	**5 *m***	3.811 ± 0.29 (1.9)	5.056 ± 0.45 (1.43)	5.944 ± 0.46 (1.22)	7.23 ± 0.51
14	**5*n***	0.444 ± 0.04 (17.7)	4.389 ± 0.40 (1.79)	1.486 ± 0.17 (5.30)	7.87 ± 0.62
15	**5o**	0.431 ± 0.03 (16.3)	2.653 ± 0.22 (2.65)	0.750 ± 0.06 (9.36)	7.02 ± 0.45
16	**5p**	6.250 ± 0.49 (3.2)	6.250 ± 0.61 (3.18)	6.383 ± 0.44 (3.12)	19.89 ± 1.21
17	**Cur**[b]	NT[d]	16.00 ± 2.04	38.25 ± 2.36	NT[d]
18	**5-FU**[c]	23.44 ± 2.09	3.15 ± 0.44	20.43 ± 1.99	—
19	**Sunitinib**	—	3.97 ± 0.32	9.67 ± 0.22	—

[a]SI (selectivity index) = IC_{50} of the normal cell line (RPE1) relative to that of the cancer cell, [b]Cur = curcumin [15,16], [c]5-FU = 5-flurouracil [15,16], [d]NT = not tested.

2.2.1.1. A431 (squamous skin) cancer cell line. All the synthesized agents **5a–p** reveal antiproliferative properties against A431 cell line with potency higher than that of 5-fluorouracil. Compounds **5k** is the most effective agent synthesized against A431 with 56.2 folds relative to 5-fluorouracil (IC_{50} = 0.417, 23.44 μM for **5k** and 5-fluorouracil, respectively). Compounds **5h**, **5n** and **5o** also reveal high efficacy against the tested cell line with potency close to that of **5k** (IC_{50} = 0.431–0.472 μM). Additionally, compounds **5d**, **5e**, **5g** and **5l** show considerable properties with sub-micromolar potencies (IC_{50} = 0.639–0.986 μM).

Based on the antiproliferative properties notable SARs (structure-activity relationships) could be attained. Attachment of the salicylate ring with a chlorine atom/substituent enhances the observed anti-proliferation properties (compound **5i** is an exception). The number of methoxy groups attached to the exocyclic benzylidene system is also a controlling factor for the exhibited bio-properties. The high number of methoxy groups, the higher potency of the tested agent as revealed by compounds **5f**/**5g**/**5h** (IC_{50} = 6.042, 0.973, 0.472 μM for **5f**, **5g** and **5h**, respectively) and **5m**/**5n**/**5o** (IC_{50} = 3.811, 0.444, 0.431 μM for **5m**, **5n** and **5o**, respectively).

2.2.1.2. MCF7 (breast) cancer cell line. Compounds **5o** and **5c** are the most potent agents synthesized against MCF7 cell line with 1.19, 1.12 folds relative to the standard reference, 5-fluorouracil (IC_{50} = 2.653, 2.806, 3.15 μM for **5o**, **5c** and 5-fluorouracil, respectively). SAR can be concluded due to the antiproliferative bio-observations. It is noticed that the 5-chlorosalicylate-containing compounds show better antiproliferative properties than the unsubstituted analogues (compounds **5c** and **5i** are exceptions). It is also noticed that, increment the number of methoxy groups attached to the benzylidene ring is associated with enhancement of the shown bio-efficacies as shown by compounds **5f**/**5g**/**5h** and **5m**/**5n**/**5o**.

2.2.1.3. HCT116 (colon) cancer cell line. Many of the synthesized piperidone-salicylate conjugates show remarkable antiproliferative properties against HCT116 (colon) cancer cell line. Compounds **5o** and **5c** are the most effective agents with sub-micromolar values (IC_{50} = 0.750, 0.986 μM for **5o** and **5c**, respectively) and 12.9, 9.8 folds relative to Sunitinib (IC_{50} = 9.67 μM), the clinically approved drug against gastrointestinal cancer. Compounds **5h**, **5l** and **5n** also reveal high potency against HCT116 cell line (IC_{50} = 1.153–1.486 μM i.e. 8.4–6.5 folds of Sunitinb). Also, conjugates **5d**, **5e**, **5g**, **5j** and **5k** show promising activity against the tested cell line (IC_{50} = 1.972–3.597 μM).

SAR due to the exhibited bio-properties strengthens the role of chloro-substituted salicylate over the unsubstituted analogues for the antiproliferation enhancement (compound **5p** is an exception). Increment in the number of methoxy group attached to the exocyclic benzylidenes of the piperidinyl heterocycle at the 3- and 5-positions are also associated in the enhancement of the antiproliferation properties as shown by compounds **5f**/**5g**/**5h** (IC_{50} = 6.083, 2.389, 1.333 μM for **5f**, **5g** and **5h**, respectively) and **5m**/**5n**/**5o** (IC_{50} = 5.944, 1.486, 0.750 μM for **5m**, **5n** and **5o**, respectively). Surprisingly, high compatibility was noticed due to the SARs of all the tested cell lines.

Safe profile of the potent agents was established upon testing against RPE1 (non-cancer, retinal pigment epithelium) cell line (Table 1).

2.2.2. Cell cycle analysis

Flow cytometric analysis is an accessible and rapid technique used intensively in medicinal chemical studies for assigning the cell cycle progress of living cells. The detected fluorescence levels estimate quantitatively the DNA content hence; determine the progress of cell cycle [79,84]. Compounds **5c** and **5o** (the most promising agents synthesized with high potency against HCT116) were selected for flow cytometric analysis studies applying the IC_{50} value of each respective agent observed through MTT bio-assay, to identify their impact on the progress of cell cycle and accessibility for induction of apoptosis and/or necrosis.

From the results obtained (Table 2, Figs. 3, 4) it is noticeable that compound **5c** arrests the cell cycle progression at G1-phase due to accumulation of DNA content at G0-G1 phase (55.28 %). Meanwhile, compound **5o** and Sunitinib (standard reference) are noticed to arrest the proliferative cells at S-phase (% DNA content = 53.11, 46.23 for **5o** and Sunitinib, respectively). Additionally, high increment in Pre-G1 phase is observed by all the tested compounds and standard reference relative to the control (% DNA content = 1.66, 44.28, 35.75, 31.69 for control, **5c**, **5o** and Sunitinib, respectively). However, decrease in G2/M phase is noticed by the synthesized agents and Sunitinib compared with control (% DNA content = 9.91, 3.59, 4.14, 7.59 for control, **5c**, **5o** and Sunitinib, respectively).

It has also been noticed that compound **5c** is a highly inducer of apoptosis and affording necrosis (% apoptosis and necrosis = 44.28, 13.41, respectively). Compound **5o** and Sunitinib are also apoptosis

Table 2
% Cell distribution of compounds **5c**, **5o** and Sunitinib for HCT116 (colon cancer cell line) by PI-flow cytometry.

Entry	Compd.	DNA content (%)			
		G0-G1	S	G2/M	Pre-G1
1	**Control**	51.38	38.71	9.91	1.66
2	**5c**	55.28	41.13	3.59	44.28
3	**5o**	42.75	53.11	4.14	35.75
4	**Sunitinib**	46.18	46.23	7.59	31.69

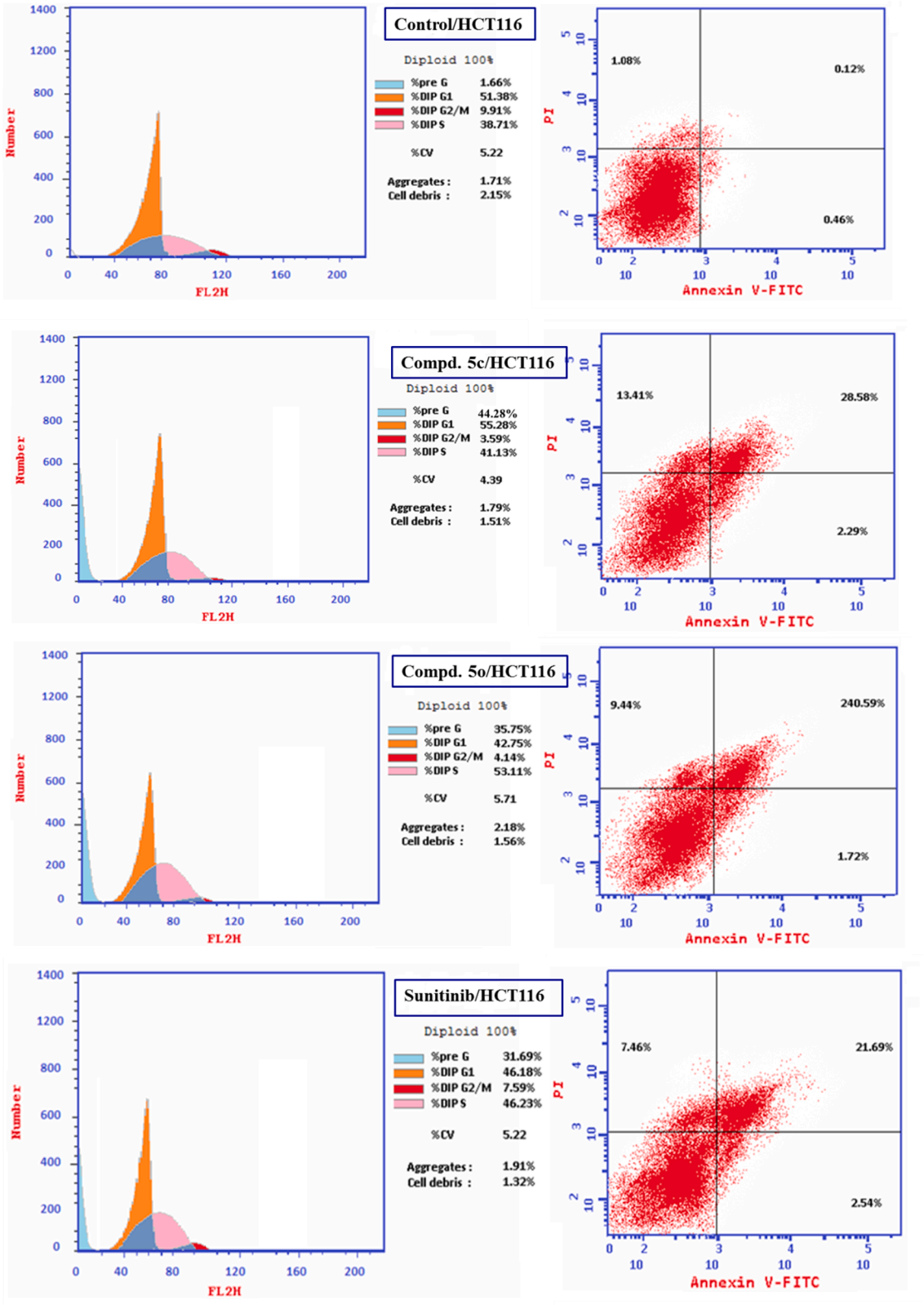

Fig. 3. Cell cycle analysis of compounds **5c**, **5o**, Sunitinib and control experiment for HCT116 (colon cancer cell line).

inducers and necrosis producers however, with lower efficiencies than compound **5c** (% apoptosis and necrosis = 35.75, 9.44; 31.69, 7.46 by compound **5o** and Sunitinib, respectively). Late stage of apoptosis is also shown by compound **5c** higher than that of compound **5o** and Sunitinib (% late stage apoptosis = 28.58, 24.59, 21.69 by compounds **5c**, **5o** and Sunitinib, respectively) (Table 3, Fig. 5).

2.2.3. *Anti-SARS-CoV-2 properties*

The anti-SARS-CoV-2 properties of the synthesized aspirin-curcumin mimic conjugates were determined by the standard technique (Table 4,

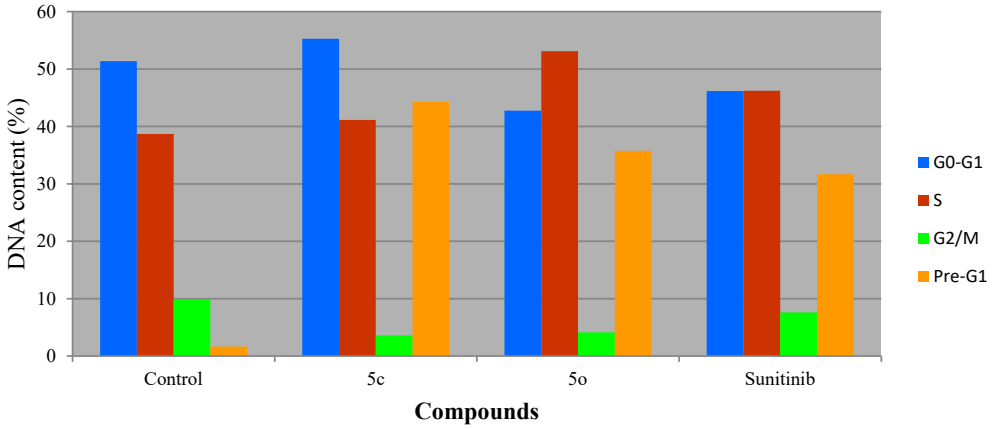

Fig. 4. DNA content of HCT116 (colon cancer cell line) PI-flow cytometry cell cycle analysis for compounds **5c**, **5o**, Sunitinib and control.

Table 3
% Apoptosis and necrosis of HCT116 (colon cancer cell line) for compounds **5c**, **5o**, Sunitinib and control.

Entry	Compd.	Apoptosis (%)			Necrosis (%)
		Total	Early	Late	
1	**Control**	1.66	0.46	0.12	1.08
2	**5c**	44.28	2.29	28.58	13.41
3	**5o**	35.75	1.72	24.59	9.44
4	**Sunitinib**	31.69	2.54	21.69	7.46

Fig. 6) [79,85,86]. Generally, all the synthesized agents (compounds **5c**, **5f** and **5j** are exceptions) show potent anti-SARS-CoV-2 properties (IC_{50} = 1.659–8.828 μM) relative to the standard references used (IC_{50} = 36.92, 24.98 μM for hydroxychloroquine and chloroquine, respectively). Compounds **5d**, **5e** and **5o** are the most effective agents synthesized with promising selectivity/therapeutic index (SI) (IC_{50} = 1.659–1.765 μM, SI = 34.0–54.7). Compounds **5p** and **5i** which contain thienylidene heterocycle exhibit remarkable therapeutic index due to high CC_{50} relative to their IC_{50} values (IC_{50} = 8.828, 3.316 μM; CC_{50} = 206.2, 416.5 μM; SI = 233.6, 125.6, for compounds **5p** and **5i**, respectively). Compound **5m** is also with high selectivity index (SI = 138.7). It has also been noticed that the increment of methoxy group(s) attached to the exocyclic benzylidenes at the 3- and 5-positions of the piperidone heyerocycle is associated with higher anti-SARS-CoV-2 potency (compound **5n** is an exception) as shown by compounds **5f**/**5g**/**5h** (IC_{50} = 149.3, 4.079, 2.236 μM) and compounds **5m**/**5o** (IC_{50} = 4.173, 1.690 μM).

2.2.4. *Tyrosine kinase inhibitory properties*

Targeted cancer chemotherapy is an important approach for competing cancer adopted intensively for reducing the side effects of other agents that many interfere with crucial cellular processes/targets or mistargeting the aimed protein/receptor [87,88]. Tyrosine kinases are classes of proteins participate in many biochemical activities controlling diverse cellular processes of which cell proliferation, differentiation and death [89]. Overexpression of protein kinases may lead to tumor invasion or metastasis. This explains the interest in tyrosine kinase inhibitors as chemotherapeutical agents. Tyrosine kinases usually classify to receptor and non-receptor tyrosine kinases. The receptor tyrosine kinases include many growth factors of which vascular endothelial growth factor (VEGF) and epidermal growth factor (EGF) that constitute important targets for developing antitumor drugs [89].

Multi-targeted tyrosine kinase inhibitors can be more potent, wider applicable agents against different cancer types and achieve satisfactory therapeutic effects [90]. Since, cancer initiation and progression usually depends on several receptor or singling pathways, the multi-targeted agents seem more appropriate with several advantages over the mono-targeted therapies [91].

2.2.4.1. VEGR-2 inhibitory properties. Angiogenesis (formation of new blood vessels from the pre-existing ones) is a physiological key for many solid tumor proliferation and metastasis. VEGF which is secreted by the malignant tumor plays an important role in the angiogenic process [92]. Three main types have been identified for vascular endothelial growth factor receptors; VEGFR-1, VEGFR-2, and VEGFR-3 which are cell surface protein modulating angiogenesis tyrosine kinase receptors [93–95]. VEGFR-2 is identified as the main receptor suppressing angiogenesis and

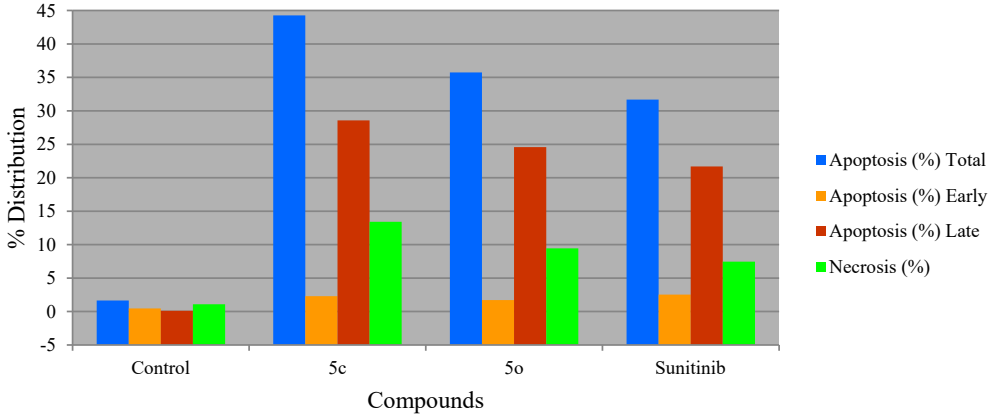

Fig. 5. % Apoptosis and necrosis of HCT116 (colon cancer cell line) for compounds **5c**, **5o**, Sunitinib and control.

Table 4
Antiviral properties of the synthesized conjugates and standard references (hydroxychloroquine and chloroquine) against SARS-CoV-2.

Entry	Compd.	IC_{50} (μM)[a]	CC_{50} (μM)[b]	SI[c]
1	**5a**	4.729	87.62	18.5
2	**5b**	3.406	77.44	22.7
3	**5c**	28.37	49.54	1.7
4	**5d**	1.659	90.82	54.7
5	**5e**	1.765	66.03	37.4
6	**5f**	149.3	182.1	1.2
7	**5 g**	4.079	234.5	57.5
8	**5 h**	2.236	78.19	35.0
9	**5i**	3.316	416.5	125.6
10	**5j**	32.29	182.6	5.7
11	**5 k**	5.868	60.60	10.3
12	**5 l**	5.898	65.19	11.1
13	**5 *m***	4.173	578.6	138.7
14	**5*n***	6.596	586.2	88.9
15	**5o**	1.690	57.50	34.0
16	**5p**	8.828	2062	233.6
17	**Hydroxychloroquine**	36.92	356.4	9.7
18	**Chloroquine**	24.98	377.7	15.1

[a]IC_{50} is the concentration for 50% growth inhibition relative to the control. [b]CC_{50} is the cytotoxic concentration for 50% cell (VERO-E6) relative to the control. [c]$SI = \frac{CC_{50}}{IC_{50}}$

inhibiting solid tumor proliferation [96].

The VEGFR-2 inhibitory properties of the synthesized aspirin-curcumin mimic conjugates are represented in Table 5 utilizing the standard Western blot technique [97] at the MTT-IC_{50} values of each prepared analogue (Supplementary Fig. S53). Generally, It has been noticed that all the synthesized agents show considerable inhibitory properties against VEGFR-2 (% inhibition = 37.2–70.5, 37.2–79.0 for MCF7 and HCT116 cell lines, respectively). Compound **5l** (R = Cl, R' = 4-BrC_6H_4) reveals the highest VEGFR-2 inhibitory properties relative to the other synthesized agents for MCF7 cell line (% inhibition = 70.5). However, compound **5j** (R = Cl, R' = Ph) is the most potent inhibitor for HCT116 cell line (% inhibition = 79.0). Compounds **5a** (R = H, R' = Ph) and **5o** [R = Cl, R' = 3,4,5-$(H_3CO)_3C_6H_2$] also show promising inhibitory properties against VEGFR-2 for MCF7 cell line (% inhibition = 64.6, 63.0 for compounds **5a** and **5o**, respectively). Additionally, compounds **5b** (R = H, R' = 4-FC_6H_4), **5c** (R = H, R' = 4-ClC_6H_4), **5l** (R = Cl, R' = 4-BrC_6H_4) and **5m** (R = Cl, R' = 4-$H_3COC_6H_4$) exhibit good affinity against VEGFR-2 for HCT116 cell line (% inhibition = 70.4–76.4).

2.2.4.2. EGFR inhibitory properties. EGFR (epidermal growth factor receptor) is an important family of the *trans*-membrane tyrosine kinase receptors necessary for proliferation and development of many solid tumors including colon, breast, lung and ovarian cancers [98,99]. Small molecule EGFR inhibitors were developed clinically and approved against many cancer types [100].

Western blot technique was employed for EGFR inhibitory properties determination [101] utilizing the IC_{50} values of the synthesized agents against MCF7 and HCT116 cell lines. From the exhibited properties it is noticeable that, most of the synthesized agents reveal EGFR inhibition properties with higher potencies that that of VEGFR-2 (% inhibition = 56.8–90.3, 56.3–72.8 for MCF7 and HCT116 cell lines, respectively) (Table 5, Supplementary Fig. S54). Compound **5a** (R = H, R' = Ph) is superior with high potency for MCF7 cell line (% inhibition = 90.3). However, compound **5b** (R = H, R' = 4-FC_6H_4) is the highest EGFR inhibitor for HCT116 cell line (% inhibition = 72.8). Additionally, compounds **5b** (R = H, R' = 4-FC_6H_4), **5c** (R = H, R' = 4-ClC_6H_4) and **5f** (R = H, R' = 4-$H_3COC_6H_4$) show promising EGFR inhibitory properties for MCF7 cell line (% inhibition = 83.7, 85.6, 76.3 for **5b**, **5c** and **5f**, respectively). Compounds **5a** (R = H, R' = Ph), **5j** (R = Cl, R' = Ph) and **5m** (R = Cl, R' = 4 = $H_3COC_6H_4$) also exhibit high EGFR inhibitory properties for HCT116 (% inhibition = 68.5–69.3).

Generally, most of the tyrosine kinase inhibitory properties (VEGFR-2 and EGFR) of MCF7 and HCT116 cell lines support the antiproliferation properties discovered of the synthesized conjugates (Table 1). The slight differences due to the antiproliferation properties and tyrosine kinase inhibitory properties can be attributed to the applied conditions due to the standard techniques.

2.2.5. COX-1/2 inhibitory properties

Inflammation is a natural response due to any harmful stimuli, infection or injury to human body [102]. It is usually associated with many serious diseases of which, rheumatoid arthritis [103], asthma [104], carcinoma [105], bacterial/viral infections [106]. Biochemical oxidation of arachidonic acid leads to the formation of prostaglandins and leukotrienes. Excessive formation of the latters is associated with inflammation, fever or pain [107]. Cyclooxygenase (COX) enzymes are responsible for biochemical transformation of arachidonic acid to prostaglandins. Cyclooxygenases are of three isoforms (COX-1, −2 and −3). COX-1 is a constitutive enzyme for normal cells producing prostaglandins of many important physiological functions such as renal blood flow and gastrointestinal mucous production [108] while, COX-2 is an inducible enzyme in the endothelial cells. COX-3 is another isoform mostly present in the cerebral cortex and heart [109]. Many traditional NSAIDs such as aspirin express their action through roughly inhibition of both COX-1 and COX-2. COX-2 selective drugs are already discovered within the last few decades (e.g. Celecoxib, Rofecoxib and Valdecoxib) (Fig. 7). However, accessibility as medication is now questionable due to their serious cardiovascular side effects discovered [110]. This is why new anti-inflammatory agents with high efficacy and limited side effects are still in demand.

The COX-1/2 inhibitory properties of the synthesized agents and aspirin (standard reference) are presented in Table 6 which determined by the standard technique [111,112]. It is noticeable that all the synthesized agents show enhanced COX-1/2 properties (IC_{50} = 0.134–0.590, 0.138–2.245 μM for COX-1 and COX-2, respectively) than their parent precursor (IC_{50} = 0.688, 2.448 μM for COX-1 and COX-2 for aspirin). Compound **5d** (R = H, R' = 4-BrC_6H_4) is the most potent COX-1 inhibitor among the entire synthesized agent (IC_{50} = 0.134 μM). Additionally, compounds **5b** (R = H, R' = 4-FC_6H_4), **5f** (R = H, R' = 4-$H_3COC_6H_4$), **5h** (R = H, R' = 3,4,5-$(H_3CO)_3C_6H_2$) and **5m** (R = Cl, R' = 4-$H_3COC_6H_4$) also show promising COX-1 inhibitory properties (IC_{50} = 0.142–0.147 μM).

Many of the synthesized agents show enhanced selectivity index (SI) towards COX-2 relative to COX-1. Compound **5p** (R = Cl, R' = 2-thienyl) is the most selective agent synthesized towards COX-2 (SI = 2.065). Compounds **5i** (R = H, R' = 2-thienyl), **5k** (R = Cl, R' = 4-ClC_6H_4) and **5l** (R = Cl, R' = 4-BrC_6H_4) also reveal promising behavior (SI = 0.589, 0.578, 0.582 for **5i**, **5k** and **5l**, respectively). Similar observations are also noticed for compounds **5f** (R = H, R' = 4-$H_3COC_6H_4$), **5m** (R = Cl, R' = 4-$H_3COC_6H_4$) and **5n** [R = Cl, R' = 3,4-$(H_3CO)_2C_6H_3$] due to SI = 0.452–0.467. It has also been noticed that the chlorosalicylate-containing conjugates are of milder COX-1 inhibitory properties than the unsubstituted analogues (compounds **5j** and **5n** are exceptions).

2.3. Molecular modeling

Molecular docking studies were undertaken for validation the EGFR properties of the synthesized conjugates utilizing Discovery Studio 2.5 software (CDOCKER standard technique) [79,113]. Adoption of the EGFR properties for computational studies, are due to the promising observations revealed relative to the exhibited VEGFR-2 properties. The PDB ID: 4G5P was considered for the targeted study [114,115]. Afatinib is the co-crystallized ligand in the protein active site (clinically approved by FDA for non-small cell lung cancer on Jul. 2013) characterized by potent EGFR inhibitory properties [116,117]. CDOCKER interactions of the synthesized conjugated show that all the tested compounds obey the same alignment in the protein active site giving to hydrogen bonding

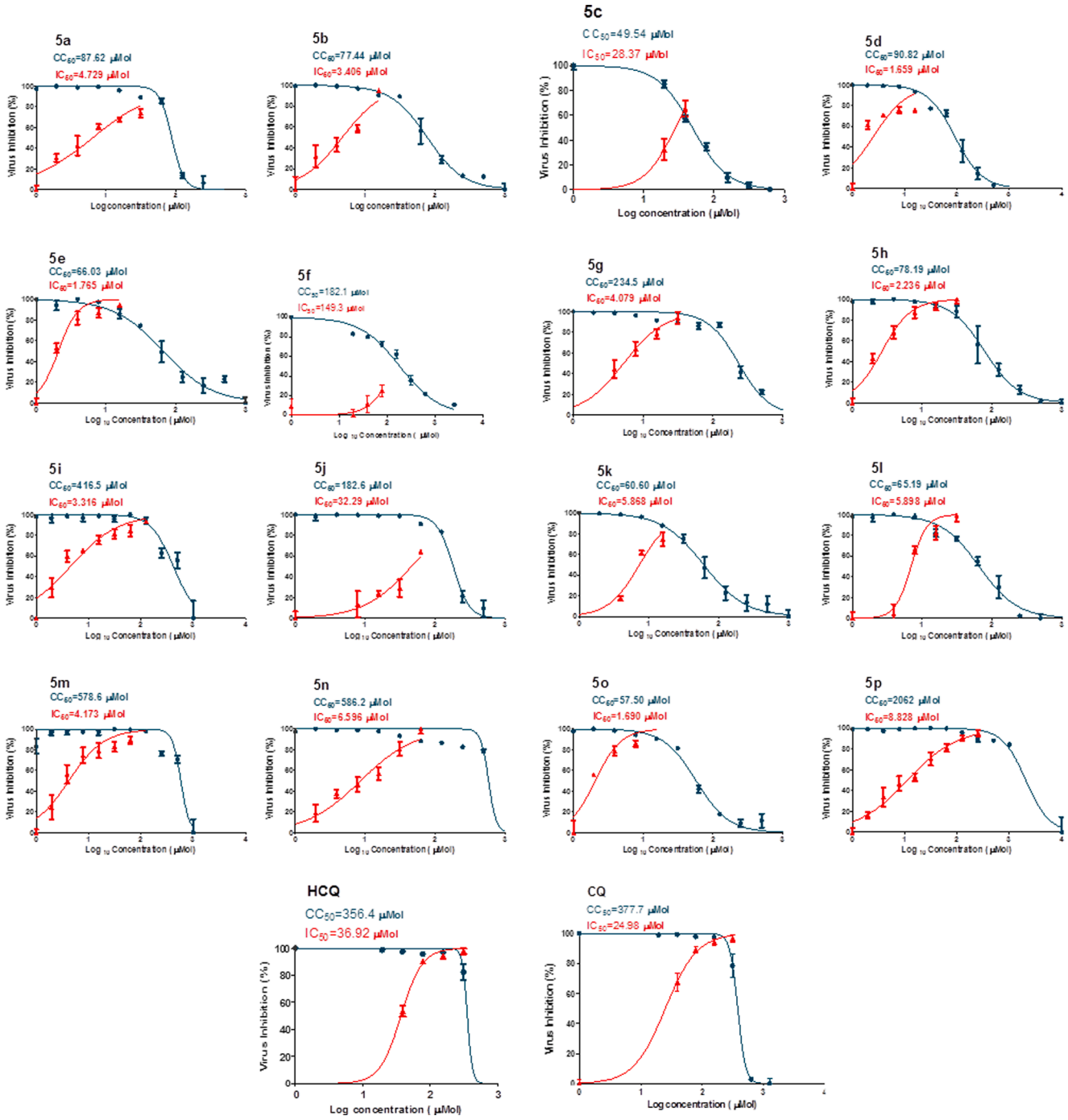

Fig. 6. Dose-response curves for the synthesized conjugates and standard references (hydroxychloroquine "HCQ", and chloroquine "CQ") against SARS-CoV-2.

interaction between the piperidinyl carbonyl oxygen (C═O) and MET793 with variable docking scores (Table 7, Supplementary Fig. S55). This behavior is comparable to that of the co-crystallized ligand (Afatinib) which exhibits two hydrogen bonding interactions taking place between the quinazolinyl *N*-1 and MET793 beside that of dimethylamino *N* and ASP800. Compound **5n** [R = Cl, R' = 3,4-$(H_3CO)_2C_6H_3$] shows additionally hydrogen bonding interaction of the acetyl carbonyl (C═O) with CYS797 beside methoxy oxygen with LYS728, explaining its relative high docking score value (-55.2 kcal mol^{-1}) among the other(s) of structural resemblance.

It has been noticed that compound **5h** [R = H, R' = 3,4,5-$(H_3CO)_3C_6H_2$] possess the highest docking score (−67.2 kcal mol^{-1}) among the entire tested conjugates and equivalent to that of the co-crystallized ligand. This computational/binding energy value can support its % inhibition EGFR values (% inhibition of EGFR = 58.9, 57.9 in MCF7 and HCT116 cell lines, respectively) and also antiproliferation properties (IC_{50} = 3.986, 1.333 µM for MCF7 and HCT116 cell lines, respectively) (Tables 1, 5). Similar noticeable data are for compound **5o** (docking score = -65.1 kcal mol^{-1}) comparable to the EGFR enzymatic inhibition (% inhibition of EGFR = 69.2, 68.2 in MCF7 and HCT116 cell lines, respectively) and antiproliferation properties (IC_{50} = 2.653, 0.750 µM for MCF7 and HCT116 cell lines, respectively). Compounds **5f** (R = H, 4-$H_3COC_6H_4$) and **5m** (R = Cl, 4-$H_3COC_6H_4$) also characterize by promising docking score values (CDOCKER scores = -53.4, −53.9 kcal mol^{-1} for **5f** and **5m**, respectively) supporting their EGFR enzymatic inhibitory properties (% inhibition = 76.3, 62.5; 62.4, 68.5 due to

Table 5
VEGFR-2 and EGFR inhibitory properties of the synthesized conjugates and 5-fluorouracil in MCF7 (breast) and HCT116 (colon) cancer cell lines.

Entry	Compd.	VEGFR2				EGFR			
		MCF7		HCT116		MCF7		HCT116	
		RQ	% Inhibition	RQ	% Inhibition	RQ	% Inhibition	RQ	% Inhibition
1	**Control**	3.725	—	3.817	—	4.226	—	4.0382	—
2	**5a**	1.32	64.6	1.24	67.5	0.41	90.3	1.24	69.3
3	**5b**	1.6	57.0	1.11	70.9	0.69	83.7	1.1	72.8
4	**5c**	1.51	59.5	1.02	73.3	0.61	85.6	1.5	62.9
5	**5d**	1.91	48.7	1.5	60.7	1.52	64.0	1.377	65.9
6	**5e**	2.202	40.9	2.209	42.1	1.707	59.6	1.664	58.8
7	**5f**	1.56	58.1	1.37	64.1	1	76.3	1.516	62.5
8	**5 g**	2.324	37.6	2.393	37.3	1.638	61.2	1.554	61.5
9	**5 h**	2.032	45.4	2.398	37.2	1.737	58.9	1.698	57.9
10	**5i**	2.000	46.3	2.297	39.8	1.540	63.6	1.564	61.3
11	**5j**	1.9	49.0	0.8	79.0	1.45	65.7	1.273	68.5
12	**5 k**	1.5	59.7	1.2	68.6	1.31	69.0	1.479	63.4
13	**5 l**	1.1	70.5	0.9	76.4	1.4	66.9	1.336	66.9
14	**5 *m***	1.966	47.2	1.13	70.4	1.59	62.4	1.273	68.5
15	**5*n***	2.338	37.2	2.389	37.4	1.825	56.8	1.610	60.1
16	**5o**	1.38	63.0	1.16	69.6	1.3	69.2	1.283	68.2
17	**5p**	2.209	40.7	2.304	39.6	1.731	59.0	1.763	56.3
18	**5-FU**	1.22	67.2	0.94	75.4	0.6	85.8	0.76	81.2

RQ = Relative quantification

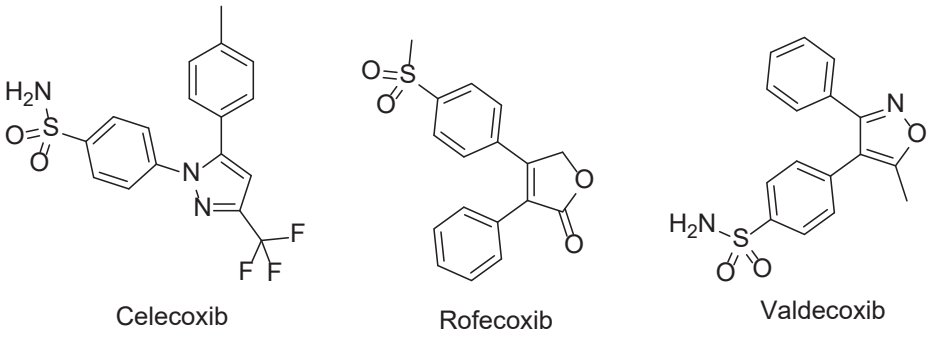

Fig. 7. Selective COX-2 inhibitors.

Table 6
COX-1 and COX-2 inhibitory properties of the synthesized agents and aspirin (standard reference).

Entry	Compd.	IC_{50}[a], μM		$SI = \frac{IC_{50(COX-1)}}{IC_{50(COX-2)}}$
		COX-1	COX-2	
1	**5a**	0.249	1.550	0.161
2	**5b**	0.146	0.442	0.330
3	**5c**	0.271	2.245	0.121
4	**5d**	0.134	1.110	0.121
5	**5e**	0.249	1.556	0.160
6	**5f**	0.147	0.315	0.467
7	**5 g**	0.262	2.176	0.120
8	**5 h**	0.147	0.438	0.336
9	**5i**	0.455	0.772	0.589
10	**5j**	0.142	1.185	0.120
11	**5 k**	0.391	0.676	0.578
12	**5 l**	0.590	1.014	0.582
13	**5 *m***	0.146	0.319	0.458
14	**5*n***	0.163	0.361	0.452
15	**5o**	0.193	1.600	0.121
16	**5p**	0.285	0.138	2.065
17	**Aspirin**	0.688	2.448	0.281

[a] IC_{50} is the concentration of a tested agent for the 50% inhibition of COX-1, COX-2.

compounds **5f** and **5m** for MCF7 and HCT116 cell lines, respectively).

Generally, the computational docking scores are correlated to the enzymatic inhibitory properties of the tested compounds. The slight differences noticed can be explained in terms of enzymatic experimental testing and theoretical/docking study techniques applied.

Table 7
CDOCKER scores of the synthesized compounds and Afatinib in PDB ID: 4G5P.

Entry	Compd.	CDOCKER interaction energy scores (kcal mol^{-1})
1	**5a**	−41.4
2	**5b**	−46.9
3	**5c**	−47.2
4	**5d**	−48.6
5	**5e**	−47.5
6	**5f**	−53.4
7	**5 g**	−52.7
8	**5 h**	−67.2
9	**5i**	−38.3
10	**5j**	−43.2
11	**5 k**	−51.6
12	**5 l**	−53.4
13	**5 *m***	−53.9
14	**5*n***	−55.2
15	**5o**	−65.1
16	**5p**	−42.9
17	**Afatinib**	−67.2

3. Conclusion

A series of piperidone-salicylate conjugates **5a–p** were synthesized in acceptable yields (60–88 %) through reaction of 3*E*, 5*E*-diylidene-4-

piperidones **4a–i** with the appropriate acid chloride of acetylsalicylic acids **3a,b** in DMF in the presence of triethylamine. All the synthesized conjugates reveal antiproliferative properties against A431 (squamous skin) cell line with potency higher than that of 5-fluorouracil. Compounds **5k** (R = Cl, R' = 4-ClC_6H_4) is the most effective agent synthesized against A431 with 56.2 folds relative to 5-fluorouracil (clinically applicable drug for colon, breast and skin cancers). Additionally, compounds **5o** [R = Cl, R' = 3,4,5- $(H_3CO)_3C_6H_2$] and **5c** (R = H, R' = 4-ClC_6H_4) are the most potent agents against MCF7 (breast) cell line with 1.19, 1.12 folds relative to the standard reference (5-fluorouracil). Compounds **5o** and **5c** also reveal remarkable potency against HCT116 (colon) cancer cell line with 12.9, 9.8 folds, respectively relative to Sunitinib (FDA approved drug against gastrointestinal cancer). Flow cytometry cell cycle analysis studies exhibit that compound **5c** arrests the cell cycle progression at G1-phase. Meanwhile, compound **5o** and Sunitinib (standard reference) are noticed to arrest the cell cycle at S-phase. Compound **5c** is a highly inducer of apoptosis and affording necrosis. Compound **5o** and Sunitinib are also apoptosis inducers and necrosis producers however, with lower efficiencies than compound **5c**. The synthesized conjugates are multi-targeted tyrosine kinase inhibitors due to the promising properties against VEGFR-2 and EGFR in MCF7 and HCT116 supporting their antiproliferation properties. Many of the synthesized agents reveal promising anti-SARS-CoV-2 properties with remarkable therapeutic index especially those containing thienylidene heterocycle. Many of the synthesized agents show enhanced COX-1/2 properties with higher selectivity index towards COX-2 relative to COX-1 than aspirin (standard reference). The possible applicability of the potent agents discovered as antitumor and anti-SARS-CoV-2 is supported by the safe profile against normal cells (RPE1 and VERO-E6).

4. Experimental

Melting points were determined on a capillary point apparatus (Stuart SMP3) equipped with a digital thermometer. IR spectra (KBr) were recorded on a Shimadzu FT-IR 8400S spectrophotometer. Reactions were monitored using thin layer chromatography (TLC) on 0.2 mm silica gel F254 plates (Merck) utilizing various solvents for elution. The chemical structures of the synthesized compounds were characterized by nuclear magnetic resonance spectra (^{1}H NMR, ^{13}C NMR) and determined on a Bruker NMR spectrometer (500 MHz, 125 MHz for ^{1}H and ^{13}C, respectively). ^{13}C NMR spectra are fully decoupled. Chemical shifts were reported in parts per million (ppm) using the deuterated solvent peak or tetramethylsilane as an internal standard.

*4.1. **Synthesis of aspirin-piperidone conjugates 5a-p** (general procedure)*

The appropriate acid chloride of aspirin **3a,b** (2.5 mmol) in DMF (5 ml) was added dropwise (within 10 min.) to a stirring solution of the corresponding piperidone **4a–i** (2.5 mmol) in DMF (15 ml) containing triethylamine (3 mmol) in an ice-cold water bath. The reaction mixture was stirred at the mentioned conditions for 4 h and stored at room temperature (20–25 °C) overnight. The separated solid upon poured into water (200 ml) containing sodium chloride (1 g) was collected, washed with tap water and crystallized from a suitable solvent affording **5a–p**.

4.1.1. 2-[3,5-Di((E)-benzylidene)-4-oxopiperidine-1-carbonyl]phenyl acetate (5a)

It was obtained from the reaction of **3a** and **4a** as pale yellow microcrystals from ethanol with mp 171–173 °C and yield 72% (0.79 g). IR: ν_{max}/cm^{-1} 1767, 1643, 1612, 1574. ^{1}H NMR (DMSO-d_6) δ (ppm): 2.14 (s, 3H, $COCH_3$), 4.58 (s, 2H, NCH_2), 5.01 (s, 2H, NCH_2), 7.01–7.04 (m, 2H, arom. H), 7.15 (dd, J = 1.5, 8.0 Hz, 1H, arom. H), 7.23–7.32 (m, 6H, arom. H), 7.49–7.68 (m, 6H, 5 arom. H + olefinic CH), 7.81 (s, 1H, olefinic CH). ^{13}C NMR (DMSO-d_6) δ (ppm): 20.4 (CH_3), 42.6 (NCH_2), 47.2 (NCH_2), 122.8, 125.7, 127.2, 128.1, 128.5, 128.9, 129.3, 129.7, 129.9, 130.3, 130.6, 132.1, 134.0, 134.3, 136.2, 136.8, 146.3 (arom. C + olefinic C), 165.6, 168.4 (CO), 185.7 (ketonic CO). Anal. Calcd. for $C_{28}H_{23}NO_4$ (437.50): C, 76.87; H, 5.30; N, 3.20. Found: C, 77.18; H, 5.49; N, 3.42.

4.1.2. 2-[3,5-Bis((E)-4-fluorobenzylidene)-4-oxopiperidine-1-carbonyl] phenyl acetate (5b)

It was obtained from the reaction of **3a** and **4b** as colorless microcrystals from light petroleum (60–80 °C) with mp 141–143 °C and yield 68% (0.80 g). IR: ν_{max}/cm^{-1} 1767, 1636, 1601, 1578. ^{1}H NMR (DMSO-d_6) δ (ppm): 2.15 (s, 3H, $COCH_3$), 4.54 (s, 2H, NCH_2), 4.99 (s, 2H, NCH_2), 7.02–7.05 (m, 2H, arom. H), 7.13–7.16 (m, 3H, arom. H), 7.29–7.39 (m, 5H, arom. H), 7.68–7.71 (m, 3H, 2 arom. H + olefinic CH), 7.79 (s, 1H, olefinic CH). ^{13}C NMR (DMSO-d_6) δ (ppm): 20.4 (CH_3), 42.5 (NCH_2), 47.0 (NCH_2), 115.3, 115.5, 115.8, 116.0, 122.8, 125.7, 127.1, 128.0, 130.2, 130.48, 130.49, 130.8, 130.82, 131.8, 131.9, 132.2, 132.3, 133.0, 133.03, 135.1, 135.7, 146.3, 161.3, 161.6, 163.3, 163.6 (arom. C + olefinic C), 165.6, 168.4 (CO), 185.5 (ketonic CO). Anal. Calcd. for $C_{28}H_{21}F_2NO_4$ (473.48): C, 71.03; H, 4.47; N, 2.96. Found: C, 71.20; H, 4.73; N, 3.14.

4.1.3. 2-[3,5-Bis((E)-4-chlorobenzylidene)-4-oxopiperidine-1-carbonyl] phenyl acetate (5c)

It was obtained from the reaction of **3a** and **4c** as yellow microcrystals from methanol with mp 173–175 °C and yield 69% (0.87 g). IR: ν_{max}/cm^{-1} 1767, 1619, 1612, 1574. ^{1}H NMR (DMSO-d_6) δ (ppm): 1.88 (s, 3H, $COCH_3$), 4.79 (s, 4H, 2 NCH_2), 7.03–7.67 (m, 14H, 12 arom. H + 2 olefinic CH). ^{13}C NMR (DMSO-d_6) δ (ppm): 20.7 (CH_3), 42.1 (NCH_2), 46.7 (NCH_2), 128.8, 132.1, 132.2, 132.9, 133.0, 133.1, 134.20, 134.24, 134.7, 134.9 (arom. C + olefinic C), 168.6 (CO), 186.0 (ketonic CO). Anal. Calcd. for $C_{28}H_{21}Cl_2NO_4$ (506.38): C, 66.41; H, 4.18; N, 2.77. Found: C, 66.55; H, 4.27; N, 2.88.

4.1.4. 2-[3,5-Bis((E)-4-bromobenzylidene)-4-oxopiperidine-1-carbonyl] phenyl acetate (5d)

It was obtained from the reaction of **3a** and **4d** as colorless microcrystals from methanol with mp 204–205 °C and yield 61% (0.91 g). IR: ν_{max}/cm^{-1} 1767, 1637, 1609, 1582. ^{1}H NMR (DMSO-d_6) δ (ppm): 2.14 (s, 3H, $COCH_3$), 4.51 (s, 2H, NCH_2), 4.96 (s, 2H, NCH_2), 7.02–7.05 (m, 2H, arom. H), 7.12–7.17 (m, 3H, arom. H), 7.30 (dt, J = 1.4, 8.0 Hz, 1H, arom. H), 7.50 (d, J = 8.1 Hz, 2H, arom. H), 7.57 (d, J = 8.1 Hz, 2H, arom. H), 7.62 (s, 1H, olefinic CH), 7.73–7.74 (m, 3H, 2 arom. H + olefinic CH). ^{13}C NMR (DMSO-d_6) δ (ppm): 20.4 (CH_3), 42.5 (NCH_2), 46.9 (NCH_2), 122.7, 123.2, 125.7, 127.1, 127.9, 130.2, 131.3, 131.7, 131.8, 132.4, 132.6, 133.1, 133.4, 134.93, 134.94, 135.6, 146.2 (arom. C + olefinic C), 165.5, 168.4 (CO), 185.5 (ketonic CO). Anal. Calcd. for $C_{28}H_{21}Br_2NO_4$ (595.29): C, 56.50; H, 3.56; N, 2.35. Found: C, 56.71; H, 3.38; N, 2.58.

4.1.5. 2-[3,5-Bis((E)-4-methylbenzylidene)-4-oxopiperidine-1-carbonyl] phenyl acetate (5e)

It was obtained from the reaction of **3a** and **4e** as colorless microcrystals from ethanol with mp 150–152 °C and yield 67% (0.78 g). IR: ν_{max}/cm^{-1} 1767, 1639, 1605, 1578. ^{1}H NMR (DMSO-d_6) δ (ppm): 2.15 (s, 3H, $COCH_3$), 2.28 (s, 3H, $ArCH_3$), 2.38 (s, 3H, $ArCH_3$), 4.58 (br s, 2H, NCH_2), 4.99 (s, 2H, NCH_2), 7.04–7.07 (m, 2H, arom. H), 7.13–7.17 (m, 5H, arom. H), 7.29–7.36 (m, 3H, arom. H), 7.51 (d, J = 7.8 Hz, 2H, arom. H), 7.63 (s, 1H, olefinic CH), 7.76 (s, 1H, olefinic CH). ^{13}C NMR (DMSO-d_6) δ (ppm): 20.4 ($COCH_3$), 20.9 ($ArCH_3$), 42.5 (NCH_2), 47.3 (NCH_2), 122.8, 125.7, 127.2, 128.1, 129.1, 129.4, 130.0, 130.2, 130.6, 131.16, 131.19, 131.3, 131.5, 136.1, 136.6, 139.3, 139.6, 146.3 (arom. C + olefinic C), 165.5, 168.4 (CO), 185.5 (ketonic CO). Anal. Calcd. for $C_{30}H_{27}NO_4$ (465.55): C, 77.40; H, 5.85; N, 3.01. Found: C, 77.59; H, 5.71; N, 2.84.

4.1.6. 2-[3,5-Bis((E)-4-methoxybenzylidene)-4-oxopiperidine-1-carbonyl] phenyl acetate (5f)

It was obtained from the reaction of **3a** and **4f** as yellow microcrystals from ethanol with mp 162–163 °C and yield 81% (1.00 g). IR: ν_{max}/cm^{-1} 1771, 1639, 1601, 1566. ^{1}H NMR (DMSO-d_6) δ (ppm): 2.15 (s, 3H, $COCH_3$), 3.76 (s, 3H, OCH_3), 3.84 (s, 3H, OCH_3), 4.57 (br s, 2H, NCH_2), 4.99 (s, 2H, NCH_2), 6.88 (d, $J = 8.5$ Hz, 2H, arom. H), 7.05–7.11 (m, 4H, arom. H), 7.17 (dd, $J = 1.5$, 8.0 Hz, 1H, arom. H), 7.22 (d, $J = 8.5$ Hz, 2H, arom. H), 7.32 (dt, $J = 1.7$, 8.2 Hz, 1H, arom. H), 7.58 (d, $J = 8.5$ Hz, 2H, arom. H), 7.62 (s, 1H, olefinic CH), 7.75 (s, 1H, olefinic CH). ^{13}C NMR (DMSO-d_6) δ (ppm): 20.4 (CH_3), 42.5 (NCH_2), 47.3 (NCH_2), 55.2, (OCH_3), 55.3 (OCH_3), 114.0, 114.4, 122.8, 125.7, 126.5, 127.2, 128.1, 129.9, 130.2, 132.0, 132.6, 135.8, 136.3, 146.3, 160.1, 160.4 (arom. C + olefinic C), 165.4, 168.4 (CO), 185.3 (ketonic CO). Anal. Calcd. for $C_{30}H_{27}NO_6$ (497.55): C, 72.42; H, 5.47; N, 2.82. Found: C, 72.53; H, 5.67; N, 3.08.

4.1.7. 2-[3,5-Bis((E)-3,4-dimethoxybenzylidene)-4-oxopiperidine-1-carbonyl]phenyl acetate (5 g)

It was obtained from the reaction of **3a** and **4 g** as yellow microcrystals from methanol with mp 98–100 °C and yield 71% (0.98 g). IR: ν_{max}/cm^{-1} 1767, 1639, 1597, 1582. ^{1}H NMR (DMSO-d_6) δ (ppm): 2.16 (s, 3H, $COCH_3$), 3.66 (s, 3H, OCH_3), 3.77 (s, 3H, OCH_3), 3.84 (s, 3H, OCH_3), 3.843 (s, 3H, OCH_3), 4.63 (br s, 2H, NCH_2), 5.01 (s, 2H, NCH_2), 6.84–6.92 (m, 3H, arom. H), 7.08–7.12 (m, 3H, arom. H), 7.18–7.23 (m, 3H, arom. H), 7.35 (dt, $J = 1.6$, 8.0 Hz, 1H, arom. H), 7.61 (s, 1H, olefinic CH), 7.77 (s, 1H, olefinic CH). ^{13}C NMR (DMSO-d_6) δ (ppm): 20.4 (CH_3), 42.2 (NCH_2), 47.5 (NCH_2), 55.3, (OCH_3), 55.5 (OCH_3), 55.53 (OCH_3), 55.58 (OCH_3), 111.5, 111.7, 113.2, 114.4, 122.8, 123.8, 124.3, 125.8, 126.8, 127.0, 127.3, 128.4, 129.8, 130.1, 130.3, 136.2, 136.7, 146.3, 148.4, 148.6, 150.0, 150.2 (arom. C + olefinic C), 165.5, 168.5 (CO), 185.2 (ketonic CO). Anal. Calcd. for $C_{32}H_{31}NO_8$ (557.60): C, 68.93; H, 5.60; N, 2.51. Found: C, 68.67; H, 5.42; N, 2.65.

4.1.8. 2-[4-Oxo-3,5-bis((E)-3,4,5-trimethoxybenzylidene)piperidine-1-carbonyl]phenyl acetate (5 h)

It was obtained from the reaction of **3a** and **4 h** as colorless microcrystals from methanol with mp 169–171 °C and yield 73% (1.12 g). IR: ν_{max}/cm^{-1} 1759, 1643, 1616, 1582. ^{1}H NMR (DMSO-d_6) δ (ppm): 2.15 (s, 3H, $COCH_3$), 3.68 (s, 3H, OCH_3), 3.69 (s, 6H, 2 OCH_3), 3.75 (s, 3H, OCH_3), 3.87 (s, 6H, 2 OCH_3), 4.65 (br s, 2H, NCH_2), 5.02 (s, 2H, NCH_2), 6.58 (s, 2H, arom. H), 6.94 (s, 2H, arom. H), 7.08–7.11 (m, 2H, arom. H), 7.22 (dd, $J = 1.5$, 7.9 Hz, 1H, arom. H), 7.35 (dt, $J = 1.5$, 8.0 Hz, 1H, arom. H), 7.60 (s, 1H, olefinic CH), 7.76 (s, 1H, olefinic CH). ^{13}C NMR (DMSO-d_6) δ (ppm): 20.4 (CH_3), 42.0 (NCH_2), 47.4 (NCH_2), 55.8, (OCH_3), 56.1 (OCH_3), 60.0 (OCH_3), 60.1 (OCH_3), 107.9, 108.1, 122.8, 125.7, 127.2, 128.5, 129.5, 129.8, 130.3, 131.2, 131.3, 136.4, 137.0, 138.7, 138.9, 146.3, 152.6, 152.9 (arom. C + olefinic C), 165.6, 168.6 (CO), 185.5 (ketonic CO). Anal. Calcd. for $C_{34}H_{35}NO_{10}$ (617.65): C, 66.12; H, 5.71; N, 2.27. Found: C, 66.29; H, 5.85; N, 2.54.

4.1.9. 2-[(3E,5E)-4-Oxo-3,5-bis(thiophen-2-ylmethylene)piperidine-1-carbonyl]phenyl acetate (5i)

It was obtained from the reaction of **3a** and **4i** as yellow microcrystals from methanol with mp 206–207 °C and yield 76% (0.85 g). IR: ν_{max}/cm^{-1} 1767, 1643, 1589, 1562. ^{1}H NMR (DMSO-d_6) δ (ppm): 2.13 (s, 3H, $COCH_3$), 4.64 (s, 2H, NCH_2), 5.07 (br s, 2H, NCH_2), 7.16–7.19 (m, 2H, arom. H), 7.24 (dt, $J = 0.7$, 7.9 Hz, 1H, arom. H), 7.32 (t, $J = 4.3$ Hz, 1H, arom. H), 7.36 (dd, $J = 1.5$, 7.6 Hz, 1H, arom. H), 7.44 (dt, $J = 1.3$, 8.2 Hz, 1H, arom. H), 7.49 (d, $J = 3.1$ Hz, 1H, arom. H), 7.70 (d, $J = 3.2$ Hz, 1H, arom. H), 7.82 (d, $J = 4.9$ Hz, 1H, arom. H), 7.86 (s, 1H, olefinic CH), 7.98 (s, 1H, olefinic CH), 8.01 (d, $J = 4.9$ Hz, 1H, arom. H). ^{13}C NMR (DMSO-d_6) δ (ppm): 20.3 (CH_3), 42.0 (NCH_2), 47.2 (NCH_2), 122.9, 126.0, 127.5, 128.2, 128.24, 128.3, 128.52, 128.54, 128.8, 130.5, 132.3, 132.5, 134.8, 137.2, 137.4, 146.4 (arom. C + olefinic C), 165.7, 168.3 (CO), 184.3 (ketonic CO). Anal. Calcd. for $C_{24}H_{19}NO_4S_2$ (449.54): C, 64.12; H, 4.26; N, 3.12. Found: C, 63.99; H, 4.11; N, 3.23.

4.1.10. 4-Chloro-2-[3,5-di((E)-benzylidene)-4-oxopiperidine-1-carbonyl] phenyl acetate (5j)

It was obtained from the reaction of **3b** and **4a** as pale yellow microcrystals from *n*-butanol with mp 182–184 °C and yield 67% (0.79 g). IR: ν_{max}/cm^{-1} 1778, 1639, 1612, 1574. ^{1}H NMR (DMSO-d_6) δ (ppm): 2.15 (s, 3H, $COCH_3$), 4.56 (br s, 2H, NCH_2), 5.00 (br s, 2H, NCH_2), 7.07 (d, $J = 8.7$ Hz, 1H, arom. H), 7.24–7.26 (m, 3H, arom. H), 7.32–7.34 (m, 4H, arom. H), 7.49 (t, $J = 7.2$ Hz, 1H, arom. H), 7.55 (t, $J = 7.5$ Hz, 2H, arom. H), 7.61 (d, $J = 7.2$ Hz, 2H, arom. H), 7.69 (s, 1H, olefinic CH), 7.80 (s, 1H, olefinic CH). ^{13}C NMR (DMSO-d_6) δ (ppm): 20.3 (CH_3), 42.6 (NCH_2), 47.0 (NCH_2), 124.7, 126.8, 128.4, 128.8, 129.3, 129.6, 129.78, 129.82, 129.96, 130.0, 130.5, 131.8, 131.9, 133.8, 134.2, 136.2, 136.8, 144.9 (arom. C + olefinic C), 164.0, 168.2 (CO), 185.5 (ketonic CO). Anal. Calcd. for $C_{28}H_{22}ClNO_4$ (471.94): C, 71.26; H, 4.70; N, 2.97. Found: C, 71.06; H, 4.49; N, 2.78.

4.1.11. 2-[3,5-Bis((E)-4-chlorobenzylidene)-4-oxopiperidine-1-carbonyl]-4-chlorophenyl acetate (5 k)

It was obtained from the reaction of **3b** and **4c** as yellow microcrystals from ethanol with mp 169–170 °C and yield 88% (1.19 g). IR: ν_{max}/cm^{-1} 1778, 1643, 1612, 1585. ^{1}H NMR (DMSO-d_6) δ (ppm): 2.15 (s, 3H, $COCH_3$), 4.51 (br s, 2H, NCH_2), 4.97 (br s, 2H, NCH_2), 7.09 (d, $J = 8.7$ Hz, 1H, arom. H), 7.23 (d, $J = 2.6$ Hz, 1H, arom. H), 7.27 (d, $J = 8.2$ Hz, 2H, arom. H), 7.34 (dd, $J = 2.6$, 8.8 Hz, 1H, arom. H), 7.38 (d, $J = 8.2$ Hz, 2H, arom. H), 7.59–7.65 (m, 5H, 4 arom. H + olefinic CH), 7.76 (s, 1H, olefinic CH). ^{13}C NMR (DMSO-d_6) δ (ppm): 20.3 (CH_3), 42.6 (NCH_2), 46.8 (NCH_2), 124.8, 126.8, 128.4, 128.9, 129.7, 129.96, 129.99, 131.5, 132.3, 132.4, 132.6, 133.0, 134.0, 134.4, 134.9, 135.6, 144.9 (arom. C + olefinic C), 164.0, 168.2 (CO), 185.4 (ketonic CO). Anal. Calcd. for $C_{28}H_{20}Cl_3NO_4$ (540.82): C, 62.18; H, 3.73; N, 2.59. Found: C, 62.09; H, 3.62; N, 2.73.

4.1.12. 2-[3,5-Bis((E)-4-bromobenzylidene)-4-oxopiperidine-1-carbonyl]-4-chlorophenyl acetate (5 l)

It was obtained from the reaction of **3b** and **4d** as yellow microcrystals from *n*-butanol with mp 172–173 °C and yield 84% (1.32 g). IR: ν_{max}/cm^{-1} 1759, 1647, 1612, 1582. ^{1}H NMR (DMSO-d_6) δ (ppm): 2.15 (s, 3H, $COCH_3$), 4.50 (br s, 2H, NCH_2), 4.96 (br s, 2H, NCH_2), 7.09 (d, $J = 8.7$ Hz, 1H, arom. H), 7.19 (d, $J = 8.2$ Hz, 2H, arom. H), 7.23 (d, $J = 2.6$ Hz, 1H, arom. H), 7.34 (dd, $J = 2.6$, 8.7 Hz, 1H, arom. H), 7.51 (d, $J = 8.2$ Hz, 2H, arom. H), 7.57 (d, $J = 8.3$ Hz, 2H, arom. H), 7.63 (s, 1H, olefinic CH), 7.73 (s, 1H, olefinic CH), 7.74 (br s, 2H, arom. H). ^{13}C NMR (DMSO-d_6) δ (ppm): 20.3 (CH_3), 42.6 (NCH_2), 46.8 (NCH_2), 122.8, 123.2, 124.8, 126.8, 129.7, 129.95, 130.0, 131.3, 131.7, 131.8, 132.4, 132.5, 132.9, 133.3, 135.0, 135.7, 144.9 (arom. C + olefinic C), 164.0, 168.2 (CO), 185.4 (ketonic CO). Anal. Calcd. for $C_{28}H_{20}Br_2ClNO_4$ (629.73): C, 53.41; H, 3.20; N, 2.22. Found: C, 53.60; H, 3.33; N, 2.47.

4.1.13. 2-[3,5-Bis((E)-4-methoxybenzylidene)-4-oxopiperidine-1-carbonyl]-4-chlorophenyl acetate (5 m)

It was obtained from the reaction of **3b** and **4f** as yellow microcrystals from *n*-butanol with mp 175–176 °C and yield 87% (1.16 g). IR: ν_{max}/cm^{-1} 1763, 1647, 1605, 1566. ^{1}H NMR (DMSO-d_6) δ (ppm): 2.15 (s, 3H, $COCH_3$), 3.78 (s, 3H, OCH_3), 3.84 (s, 3H, OCH_3), 4.56 (br s, 2H, NCH_2), 4.98 (s, 2H, NCH_2), 6.89 (d, $J = 8.4$ Hz, 2H, arom. H), 7.09–7.13 (m, 3H, arom. H), 7.23 (d, $J = 8.4$ Hz, 2H, arom. H), 7.26 (d, $J = 2.6$ Hz, 1H, arom. H), 7.37 (dd, $J = 2.6$, 8.7 Hz, 1H, arom. H), 7.58 (d, $J = 8.4$ Hz, 2H, arom. H), 7.62 (s, 1H, olefinic CH), 7.74 (s, 1H, olefinic CH). ^{13}C NMR (DMSO-d_6) δ (ppm): 20.3 (CH_3), 42.6 (NCH_2), 47.2 (NCH_2), 55.3 (OCH_3), 114.0, 114.4, 124.8, 126.4, 126.8, 126.9, 129.76, 129.78, 129.9, 130.01, 130.03, 132.0, 132.6, 135.9, 136.5, 145.0, 160.1, 160.4 (arom. C + olefinic C), 163.9, 168.2 (CO), 185.2 (ketonic CO). Anal. Calcd. for $C_{30}H_{26}ClNO_6$ (531.99): C, 67.73; H, 4.93; N, 2.63. Found: C, 67.49; H, 5.12; N, 2.46.

4.1.14. 2-[3,5-Bis((E)-3,4-dimethoxybenzylidene)-4-oxopiperidine-1-carbonyl]-4-chlorophenyl acetate (5n)

It was obtained from the reaction of **3b** and **4 g** as yellow microcrystals from *n*-butanol with mp 173–175 °C and yield 61% (0.90 g). IR: ν_{max}/cm^{-1} 1767, 1647, 1582, 1516. ^{1}H NMR (DMSO-d_6) δ (ppm): 2.15 (s, 3H, $COCH_3$), 3.69 (s, 3H, OCH_3), 3.78 (s, 3H, OCH_3), 3.84 (s, 3H, OCH_3), 3.85 (s, 3H, OCH_3), 4.62 (br s, 2H, NCH_2), 4.99 (s, 2H, NCH_2), 6.86–6.94 (m, 3H, arom. H), 7.11–7.23 (m, 4H, arom. H), 7.31 (d, J = 2.6 Hz, 1H, arom. H), 7.39 (dd, J = 2.6, 8.7 Hz, 1H, arom. H), 7.61 (s, 1H, olefinic CH), 7.75 (s, 1H, olefinic CH). ^{13}C NMR (DMSO-d_6) δ (ppm): 20.3 (CH_3), 42.4 (NCH_2), 47.3 (NCH_2), 55.2, 55.49, 55.53, 55.6 (OCH_3), 111.5, 111.7, 113.1, 114.4, 123.8, 124.2, 124.8, 126.6, 126.9, 127.0, 129.7, 129.9, 130.03, 130.05, 130.14, 136.3, 136.8, 145.0, 148.3, 148.6, 150.0, 150.2 (arom. C + olefinic C), 163.9, 168.3 (CO), 185.1 (ketonic CO). Anal. Calcd. for $C_{32}H_{30}ClNO_8$ (592.04): C, 64.92; H, 5.11; N, 2.37. Found: C, 65.08; H, 5.03; N, 2.33.

4.1.15. 4-Chloro-2-(4-oxo-3,5-bis((E)-3,4,5-trimethoxybenzylidene) piperidine-1-carbonyl)phenyl acetate (5o)

It was obtained from the reaction of **3b** and **4 h** as yellow microcrystals from *n*-butanol with mp 148–150 °C and yield 60% (0.98 g). IR: ν_{max}/cm^{-1} 1763, 1647, 1609, 1578. ^{1}H NMR (DMSO-d_6) δ (ppm): 2.15 (s, 3H, $COCH_3$), 3.69 (s, 3H, OCH_3), 3.71 (s, 6H, 2 OCH_3), 3.75 (s, 3H, OCH_3), 3.86 (s, 6H, 2 OCH_3), 4.64 (br s, 2H, NCH_2), 5.01 (s, 2H, NCH_2), 6.59 (s, 2H, arom. H), 6.93 (s, 2H, arom. H), 7.15 (d, J = 8.7 Hz, 1H, arom. H), 7.31 (d, J = 2.7 Hz, 1H, arom. H), 7.38 (dd, J = 2.6, 8.7 Hz, 1H, arom. H), 7.61 (s, 1H, olefinic CH), 7.75 (s, 1H, olefinic CH). ^{13}C NMR (DMSO-d_6) δ (ppm): 20.3 (CH_3), 42.1 (NCH_2), 47.2 (NCH_2), 55.7, 56.1, 59.9, 60.1 (OCH_3), 107.8, 108.1, 124.8, 126.7, 129.3, 129.7, 130.0, 130.3, 131.0, 131.1, 136.4, 137.1, 138.7, 138.9, 145.1, 152.5, 152.9 (arom. C + olefinic C), 164.0, 168.5 (CO), 185.4 (ketonic CO). Anal. Calcd. for $C_{34}H_{34}ClNO_{10}$ (652.09): C, 62.63; H, 5.26; N, 2.15. Found: C, 62.40; H, 5.39; N, 1.97.

4.1.16. 4-Chloro-2-[(3E,5E)-4-oxo-3,5-bis(thiophen-2-ylmethylene) piperidine-1-carbonyl]phenyl acetate (5p)

It was obtained from the reaction of **3b** and **4i** as yellow microcrystals from *n*-butanol with mp 188–190 °C and yield 75% (0.91 g). IR: ν_{max}/cm^{-1} 1767, 1643, 1589, 1562. ^{1}H NMR (DMSO-d_6) δ (ppm): 2.14 (s, 3H, $COCH_3$), 4.64 (br s, 2H, NCH_2), 5.04 (br s, 2H, NCH_2), 7.19 (t, J = 4.4 Hz, 1H, arom. H), 7.24 (d, J = 8.4 Hz, 1H, arom. H), 7.32 (t, J = 4.4 Hz, 1H, arom. H), 7.48–7.53 (m, 3H, arom. H), 7.70 (d, J = 3.7 Hz, 1H, arom. H), 7.85 (d, J = 5.1 Hz, 1H, arom. H), 7.88 (s, 1H, olefinic CH), 7.98 (s, 1H, olefinic CH), 8.02 (d, J = 5.1 Hz, 1H, arom. H). ^{13}C NMR (DMSO-d_6) δ (ppm): 20.3 (CH_3), 42.1 (NCH_2), 47.0 (NCH_2), 124.9, 127.3, 127.9, 128.2, 128.3, 128.4, 128.5, 128.9, 130.0, 130.27, 130.31, 132.3, 132.6, 134.86, 134.98, 137.1, 137.4, 145.2 (arom. C + olefinic C), 164.1, 168.2 (CO), 184.2 (ketonic CO). Anal. Calcd. for $C_{24}H_{18}ClNO_4S_2$ (483.98): C, 59.56; H, 3.75; N, 2.89. Found: C, 59.51; H, 3.89; N, 2.97.

4.2. Biological and molecular modeling studies

Details of the experimental techniques utilized for biological studies were mentioned in the supplementary file.

Declaration of Competing Interest

The authors declare that they have no known competing financial interests or personal relationships that could have appeared to influence the work reported in this paper.

Acknowledgment

This work was supported financially by National Research Centre, Egypt, project ID: 12060101.

Appendix A. Supplementary material

Supplementary data to this article can be found online at https://doi.org/10.1016/j.bioorg.2021.105466.

References

[1] Z. Guo, The modification of natural products for medical use, Acta Pharm. Sinica B 7 (2) (2017) 119–136, https://doi.org/10.1016/j.apsb.2016.06.003.
[2] K. Bairwa, J. Grover, M. Kania, S.M. Jachak, Recent developments in chemistry and biology of curcumin analogues, RSC Adv. 4 (2014) 13946–13978, https://doi.org/10.1039/c4ra00227j.
[3] G. Banuppriya, R. Sribalan, V. Padmini, V. Shanmugaiah, Biological evaluation and molecular docking studies of new curcuminoid derivatives: synthesis and characterization, Bioorg. Med. Chem. Lett. 26 (7) (2016) 1655–1659, https://doi.org/10.1016/j.bmcl.2016.02.066.
[4] B.C. Jordan, B. Kumar, R. Thilagavathi, A. Yadhav, P. Kumar, C. Selvam, Synthesis, evaluation of cytotoxic properties of promising curcumin analogues and investigation of possible molecular mechanisms, Chem. Biol. Drug Des. 91 (1) (2018) 332–337, https://doi.org/10.1111/cbdd.13061.
[5] C.D. Mock, B.C. Jordan, C. Selvam, Recent advances of curcumin and its analogues in breast cancer prevention and treatment, RSC Adv. 5 (92) (2015) 75575–75588, https://doi.org/10.1039/C5RA14925H.
[6] L. Zhang, L.i. Zhang, X. Cheng, Y. Gao, J. Bao, H. Yu, H. Guan, Y. Sun, R. Lu, Curcumin induces cell death of human papillary thyroid carcinoma BCPAP cells through endoplasmic reticulum stress, RSC Adv. 6 (58) (2016) 52905–52912, https://doi.org/10.1039/C6RA01515H.
[7] L. Cui, J. Miao, L. Cui, Cytotoxic effect of curcumin on malaria parasite *Plasmodium falciparum*: inhibition of histone acetylation and generation of reactive oxygen species, Antimicrob. Agents Chemothe. 51 (2) (2007) 488–494, https://doi.org/10.1128/AAC.01238-06.
[8] R.A. Sharma, H.R. McLelland, K.A. Hill, C.R. Ireson, S.A. Euden, M.M. Manson, M. Pirmohamed, L.J. Marnett, A.J. Gescher, W.P. Steward, Pharmacodynamic and pharmacokinetic study of oral *curcuma* extract in patients with colorectal cancer, Clin. Cancer Res. 7 (2001) 1894–1900.
[9] P.V. Sri Ramya, S. Angapelly, L. Guntuku, C. Singh Digwal, B. Nagendra Babu, V. G.M. Naidu, A. Kamal, Synthesis and biological evaluation of curcumin inspired indole analogues as tubulin polymerization inhibitors, Eur. J. Med. Chem. 127 (2017) 100–114, https://doi.org/10.1016/j.ejmech.2016.12.043.
[10] C. Qiu, Y. Hu, K.e. Wu, K.e. Yang, N. Wang, Y. Ma, H. Zhu, Y.i. Zhang, Y. Zhou, C. Chen, S. Li, L. Fu, X. Zhang, Z. Liu, Synthesis and biological evaluation of allylated mono-carbonyl analogues of curcumin (MACs) as anti-cancer agents for cholangiocarcinoma, Bioorg. Med. Chem. Lett. 26 (24) (2016) 5971–5976, https://doi.org/10.1016/j.bmcl.2016.10.080.
[11] P.K. Sahu, Design, structure activity relationship, cytotoxicity and evaluation of antioxidant activity of curcumin derivatives/analogues. Eur. J. Med. Chem. 121 (2016) 510–516. dx.doi.org/10.1016/j.ejmech.2016.05.037.
[12] P.V. Sri Ramya, L. Guntuku, S. Angapelly, S. Karri, C.S. Digwal, B.N. Babu, V.G. M. Naidu, A. Kamal, Curcumin inspired 2-chloro/phenoxy quinoline analogues: Synthesis and biological evaluation as potential anticancer agents, Bioorg. Med. Chem. Lett. 28 (2018) 892–898, https://doi.org/10.1016/j.bmcl.2018.01.070.
[13] M.F.F. Mohd Aluwi, K. Rullah, B.M. Yamin, S.W. Leong, M.N. Abdul Bahari, S. J. Lim, S.M. Mohd Faudzi, J. Jalil, F. Abas, N. Mohd Fauzi, N.H. Ismail, I. Jantan, K.W. Lam, Synthesis of unsymmetrical monocarbonyl curcumin analogues with potent inhibition on prostaglandin E2 production in LPS-induced murine and human macrophages cell lines, Bioorg. Med. Chem. Lett. 26 (10) (2016) 2531–2538, https://doi.org/10.1016/j.bmcl.2016.03.092.
[14] M. Patanapongpibul, C. Zhang, G. Chen, S. Guo, Q. Zhang, S. Zheng, G. Wang, Q.-H. Chen, Optimization of diarylpentadienones as chemotherapeutics for prostate cancer, Bioorg. Med. Chem. 26 (16) (2018) 4751–4760, https://doi.org/10.1016/j.bmc.2018.08.018.
[15] N.G. Fawzy, S.S. Panda, W. Fayad, E.M. Shalaby, A.M. Srour, A.S. Girgis, Synthesis, human topoisomerase IIα inhibitory properties and molecular modeling studies of anti-proliferative curcumin mimics, RSC Adv. 9 (58) (2019) 33761–33774, https://doi.org/10.1039/C9RA05661K.
[16] N.G. Fawzy, S.S. Panda, W. Fayad, M.A. El-Manawaty, A.M. Srour, A.S. Girgis, Novel curcumin inspired antineoplastic 1-sulfonyl-4-piperidones: design, synthesis and molecular modeling studies, Anti-Cancer Agents Med. Chem. 19 (8) (2019) 1069–1078, https://doi.org/10.2174/1871520619666190408131639.
[17] D. Mandalapu, K.S. Saini, S. Gupta, V. Sharma, M. Yaseen Malik, S. Chaturvedi, V. Bala, Hamidullah, S. Thakur, J.P. Maikhuri, M. Wahajuddin, R. Konwar, G. Gupta, V.L. Sharma, Synthesis and biological evaluation of some novel triazole hybrids of curcumin mimics and their selective anticancer activity against breast and prostate cancer cell lines, Bioorg. Med. Chem. Lett. 26 (17) (2016) 4223–4232, https://doi.org/10.1016/j.bmcl.2016.07.053.
[18] D. Mandalapu, D.K. Singh, S. Gupta, V.M. Balaramnavar, M. Shafiq, D. Banerjee, V.L. Sharma, Discovery of monocarbonyl curcumin hybrids as a novel class of human DNA ligase I inhibitors: *in silico* design, synthesis and biology, RSC Adv. 6 (31) (2016) 26003–26018, https://doi.org/10.1039/C5RA25853G.
[19] A.-M. Katsori, M. Chatzopoulou, K. Dimas, C. Kontogiorgis, A. Patsilinakos, T. Trangas, D. Hadjipavlou-Litina, Curcumin analogues as possible anti-proliferative & anti-inflammatory agents, Eur. J. Med. Chem. 46 (2011) 2722–2735, https://doi.org/10.1016/j.ejmech.2011.03.060.

[20] S. Bindu, S. Mazumder, U. Bandyopadhyay, Non-steroidal anti-inflammatory drugs (NSAIDs) and organ damage: a current perspective, Biochem. Pharm. 180 (2020) 114147, https://doi.org/10.1016/j.bcp.2020.114147.

[21] C. Fiala, M.D. Pasic, Aspirin: Bitter pill or miracle drug?, Clin. Biochem. 85 (2020) 1–4. dx.doi.org/10.1016/j.bmcl.2016.07.053.

[22] A.T. Collaboration, Collaborative overview of randomised trials of antiplatelet therapy. prevention of death, myocardial infarction, and stroke by prolonged antiplatelet therapy in various categories of patients, BMJ 308 (1994) 81–106, https://doi.org/10.1136/bmj.308.6921.81.

[23] L.A. García Rodríguez, S. Hernández-Díaz, F.J. de Abajo, Association between aspirin and upper gastrointestinal complications: systematic review of epidemiologic studies, Br. J. Clin. Pharmacol. 52 (2001) 563–571, https://doi.org/10.1046/j.0306-5251.2001.01476.x.

[24] C.M. Moldovan, O. Oniga, A. Pârvu, B. Tiperciuc, P. Verite, A. Pîrnău, O. Crişan, M. Bojiţă, R. Pop, Synthesis and anti-inflammatory evaluation of some new acylhydrazones bearing 2-aryl-thiazole, Eur. J. Med. Chem. 46 (2) (2011) 526–534, https://doi.org/10.1016/j.ejmech.2010.11.032.

[25] S. Derry, Y.K. Loke, Risk of gastrointestinal haemorrhage with long term use of aspirin: meta-analysis, BMJ 321 (2000) 1183–1187, https://doi.org/10.1136/bmj.321.7270.1183.

[26] R. Jirmář, P. Widimský, Enteric-coated aspirin in cardiac patients: Is it less effective than plain aspirin?, Cor Vasa 60 (2018) e165–e168. dx.doi.org/10.1016/j.crvasa.2017.05.011.

[27] K.K.F. Tsoi, J.M.W. Ho, F.C.H. Chan, J.J.Y. Sung, Long-term use of low-dose aspirin for cancer prevention: a 10-year population cohort study in Hong Kong, Int. J. Cancer 145 (1) (2019) 267–273, https://doi.org/10.1002/ijc.v145.110.1002/ijc.32083.

[28] T.G. Simon, Y. Ma, J.F. Ludvigsson, D.Q. Chong, E.L. Giovannucci, C.S. Fuchs, J. A. Meyerhardt, K.E. Corey, R.T. Chung, X. Zhang, A.T. Chan, Association between aspirin use and risk of hepatocellular carcinoma, JAMA Oncol. 4 (2018) 1683–1690, https://doi.org/10.1001/jamaoncol.2018.4154.

[29] M.E. Barnard, E.M. Poole, G.C. Curhan, A.H. Eliassen, B.A. Rosner, K.L. Terry, S. S. Tworoger, Association of analgesic use with risk of ovarian cancer in the nurses' health studies, JAMA Oncol. 4 (2018) 1675–1682, https://doi.org/10.1001/jamaoncol.2018.4149.

[30] D.A. Drew, Y. Cao, A.T. Chan, Aspirin and colorectal cancer: the promise of precision chemoprevention, Nat. Rev. Cancer. 16 (3) (2016) 173–186, https://doi.org/10.1038/nrc.2016.4.

[31] P.M. Rothwell, M. Wilson, C.-E. Elwin, B. Norrving, A. Algra, C.P. Warlow, T. W. Meade, Long-term effect of aspirin on colorectal cancer incidence and mortality: 20-year follow-up of five randomised trials, Lancet 376 (2010) 1741–1750, https://doi.org/10.1016/S0140-6736(10)61543-7.

[32] T.W. Johnson, K.E. Anderson, D. Lazovich, A.R. Folsom, Association of aspirin and nonsteroidal anti-inflammatory drug use with breast cancer, Cancer Epidemiol. Biomark. Prev. 11 (2002) 1586–1591.

[33] J. Cuzick, F. Otto, J.A. Baron, P.H. Brown, J. Burn, P. Greenwald, J. Jankowski, C. La Vecchia, F. Meyskens, H.J. Senn, M. Thun, Aspirin and non-steroidal anti-inflammatory drugs for cancer prevention: an international consensus statement, Lancet Oncol. 10 (5) (2009) 501–507, https://doi.org/10.1016/S1470-2045(09)70035-X.

[34] M.-J. Yin, Y. Yamamoto, R.B. Gaynor, The anti-inflammatory agents aspirin and salicylate inhibit the activity of IκB kinase-β, Nature 396 (1998) 77–80, https://doi.org/10.1038/23948.

[35] E. Kopp, S. Ghosh, Inhibition of NF-kappa B by sodium salicylate and aspirin, Science 265 (1994) 956–959, https://doi.org/10.1126/science.8052854.

[36] Y. Zhu, J. Fu, K.L. Shurlknight, D.N. Soroka, Y. Hu, X. Chen, S. Sang, Novel resveratrol-based aspirin prodrugs: synthesis, metabolism, and anticancer activity, J. Med. Chem. 58 (2015) 6494–6506, https://doi.org/10.1021/acs.jmedchem.5b00536.

[37] I. Kastrati, V.A. Litosh, S. Zhao, M. Alvarez, G.R.J. Thatcher, J. Frasor, A novel aspirin prodrug inhibits NFκB activity and breast cancer stem cell properties, BMC Canc. 15 (2015) 845, https://doi.org/10.1186/s12885-015-1868-7.

[38] N. Puttaswamy, G.S. Pavan Kumar, M. Al-Ghorbani, V. Vigneshwaran, B. T. Prabhakar, S.A. Khanum, Synthesis and biological evaluation of salicylic acid conjugated isoxazoline analogues on immune cell proliferation and angiogenesis, Eur. J. Med. Chem. 114 (2016) 153–161, https://doi.org/10.1016/j.ejmech.2016.02.052.

[39] F. Vannini, A.C. MacKessack-Leitch, E.K. Eschbach, M. Chattopadhyay, R. Kodela, K. Kashfi, Synthesis and anti-cancer potential of the positional isomers of NOSH-aspirin (NBS-1120) a dual nitric oxide and hydrogen sulfide releasing hybrid, Bioorg. Med. Chem. Lett. 25 (20) (2015) 4677–4682, https://doi.org/10.1016/j.bmcl.2015.08.023.

[40] R.K. Pathak, S. Marrache, J.H. Choi, T.B. Berding, S. Dhar, The prodrug platin-A: simultaneous release of cisplatin and aspirin, Angew. Chem. Int. Ed. 53 (7) (2014) 1963–1967, https://doi.org/10.1002/anie.201308899.

[41] S. Willetts, D.W. Foley, True or false? Challenges and recent highlights in the development of aspirin prodrugs, Eur. J. Med. Chem. 192 (2020) 112200, https://doi.org/10.1016/j.ejmech.2020.112200.

[42] H.-D. Chae, N. Cox, S. Capolicchio, J.W. Lee, N. Horikoshi, S. Kam, A.A. Ng, J. Edwards, T.-L. Butler, J. Chan, Y. Lee, G. Potter, M.C. Capece, C.W. Liu, S. Wakatsuki, M. Smith, K.M. Sakamoto, SAR optimization studies on modified salicylamides as a potential treatment for acute myeloid leukemia through inhibition of the CREB pathway, Bioorg. Med., Chem. Lett. 29 (16) (2019) 2307–2315, https://doi.org/10.1016/j.bmcl.2019.06.023.

[43] R. Jorda, J. Dušek, E. Řezníčková, K. Pauk, P.P. Magar, A. Imramovský, V. Kryštof, Synthesis and antiproteasomal activity of novel O-benzyl salicylamide-based inhibitors built from leucine and phenylalanine, Eur. J. Med. Chem. 135 (2017) 142–158, https://doi.org/10.1016/j.ejmech.2017.04.027.

[44] M. Zuo, Y.-W. Zheng, S.-M. Lu, Y. Li, S.-Q. Zhang, Synthesis and biological evaluation of N-aryl salicylamides with a hydroxamic acid moiety at 5-position as novel HDAC–EGFR dual inhibitors, Bioorg. Med. Chem. 20 (14) (2012) 4405–4412, https://doi.org/10.1016/j.bmc.2012.05.034.

[45] A. Pannunzio, M. Coluccia, Cyclooxygenase-1 (COX-1) and COX-1 inhibitors in cancer: a review of oncology and medicinal chemistry literature, Pharmaceuticals 11 (2018) 101, https://doi.org/10.3390/ph11040101.

[46] T. Chen, Y. Huang, J. Hong, X. Wei, F. Zeng, J. Li, G. Ye, J. Yuan, Y. Long, Preparation, COX-2 inhibition and anticancer activity of sclerotiorin derivatives, Mar. Drugs 19 (2021) 12, https://doi.org/10.3390/md19010012.

[47] R. Islam, K.W. Lam, Recent progress in small molecule agents for the targeted therapy of triple-negative breast cancer, Eur. J. Med. Chem. 207 (2020) 112812, https://doi.org/10.1016/j.ejmech.2020.112812.

[48] T. Liu, S. Song, X. Wang, J. Hao, Small-molecule inhibitors of breast cancer-related targets: potential therapeutic agents for breast cancer, Eur. J. Med. Chem. 210 (2021) 112954, https://doi.org/10.1016/j.ejmech.2020.112954.

[49] A.S. Girgis, S.S. Panda, I.S.A. Farag, A.M. El-Shabiny, A.M. Moustafa, N.S. M. Ismail, G.G. Pillai, C.S. Panda, C.D. Hall, A.R. Katritzky, Synthesis, and QSAR analysis of anti-oncological active spiro-alkaloids, Org. Biomol. Chem. 13 (6) (2015) 1741–1753, https://doi.org/10.1039/C4OB02149E.

[50] K. Wang, W. Song, Y. Shen, H. Wang, Z. Fan, LncRNA *KLK8* modulates stem cell characteristics in colon cancer, Pathol. – Res. Prac. 224 (2021) 153437, https://doi.org/10.1016/j.prp.2021.153437.

[51] S. Haraldsdottir, H.M. Einarsdottir, A. Smaradottir, A. Gunnlaugsson, T. R. Halfdanarson, Colorectal cancer – review, Laeknabladid 100 (2014) 75–82, https://doi.org/10.17992/lbl.2014.02.531.

[52] M. Ashraf-Uz-Zaman, S. Shahi, R. Akwii, M.S. Sajib, M.J. Farshbaf, R.R. Kallem, W. Putnam, W. Wang, R. Zhang, K. Alvina, P.C. Trippier, C.M. Mikelis, N. A. German, Design, synthesis and structure-activity relationship study of novel urea compounds as FGFR1 inhibitors to treat metastatic triplenegative breast cancer, Eur. J. Med. Chem. 209 (2021) 112866, https://doi.org/10.1016/j.ejmech.2020.112866.

[53] C.W.S. Tong, M. Wu, W.C.S. Cho, K.K.W. To, Recent advances in the treatment of breast cancer, Front. Oncol. 8 (2018) 227–236, https://doi.org/10.3389/fonc.2018.00227.

[54] R. Dhankhar, S.P. Vyas, A.K. Jain, S. Arora, G. Rath, A.K. Goyal, Advances in novel drug delivery strategies for breast cancer therapy, Artif. Cells Blood Substit, Immobil. Biotechnol. 38 (5) (2010) 230–249, https://doi.org/10.3109/10731199.2010.494578.

[55] Z. Apalla, D. Nashan, R.B. Weller, X. Castellsague, Skin cancer: epidemiology, disease burden, pathophysiology, diagnosis and therapeutic approaches, Dermatol. Ther. 7 (2017) 5–19, https://doi.org/10.1007/s13555-016-0165-y.

[56] D.Y. Diao, T.K. Lee, Sun-protective behaviors in populations at high risk for skin cancer, Psychol. Res. Behav. Manage. 7 (2013) 9–18, https://doi.org/10.2147/PRBM.S40457.

[57] J.S. Reis, M.A. Corrêa, C.A. Ribeirob, J.L.D. Santos, Synthesis and evaluation of 1,3,5-triazine derivatives as sunscreens useful to prevent skin cancer, Bioorg. Med. Chem. Lett. 29 (2019) 126755, https://doi.org/10.1016/j.bmcl.2019.126755.

[58] T. Roy, S.T. Boateng, S. Banang-Mbeumi, P.K. Singh, P. Basnet, R.-C.-N. Chamcheu, F. Ladu, I. Chauvin, V.S. Spiegelman, R.A. Hill, K.G. Kousoulas, B. M. Nagalo, A.L. Walker, J. Fotie, S. Murru, M. Sechi, J.C. Chamcheu, Synthesis, inverse docking-assisted identification and *in vitro* biological characterization of flavonol-based analogs of fisetin as c-Kit, CDK2 and mTOR inhibitors against melanoma and non-melanoma skin cancers, Bioorg. Chem. 107 (2021) 104595, https://doi.org/10.1016/j.bioorg.2020.104595.

[59] K. Mohamed, N. Yazdanpanah, A. Saghazadeh, N. Rezaei, Computational drug discovery and repurposing for the treatment of COVID-19: a systematic review, Bioorg. Chem. 106 (2021) 104490, https://doi.org/10.1016/j.bioorg.2020.104490.

[60] L. Zheng, L. Zhang, J. Huang, K.S. Nandakumar, S. Liu, K. Cheng, Potential treatment methods targeting 2019-nCoV infection, Eur. J. Med. Chem. 205 (2020) 112687, https://doi.org/10.1016/j.ejmech.2020.112687.

[61] https://covid19.who.int/ (accessed on Sept. 23, 2021).

[62] M. Negi, P.A. Chawla, A. Faruk, V. Chawla, Role of heterocyclic compounds in SARS and SARS CoV-2 pandemic, Bioorg. Chem. 104 (2020) 104315, https://doi.org/10.1016/j.bioorg.2020.104315.

[63] D. Kumar, G. Chauhan, S. Kalra, B. Kumar, M.S. Gill, A perspective on potential target proteins of COVID-19: comparison with SARS-CoV for designing new small molecules, Bioorg. Chem. 104 (2020) 104326, https://doi.org/10.1016/j.bioorg.2020.104326.

[64] S.A. Amin, S. Banerjee, K. Ghosh, S. Gayen, T. Jha, Protease targeted COVID-19 drug discovery and its challenges: insight into viral main protease (Mpro) and papain-like protease (PLpro) inhibitors, Bioorg. Med. Chem. 29 (2021) 115860, https://doi.org/10.1016/j.bmc.2020.115860.

[65] J.L. Vique-Sánchez, Potential inhibitors interacting in Neuropilin-1 to develop an adjuvant drug against COVID-19, by molecular docking, Bioorg. Med. Chem. 33 (2021) 116040, https://doi.org/10.1016/j.bmc.2021.116040.

[66] I. Shagufta, Ahmad, The race to treat COVID-19: potential therapeutic agents for the prevention and treatment of SARS-CoV-2, Eur. J. Med. Chem. 213 (2021) 113157, https://doi.org/10.1016/j.ejmech.2021.113157.

[67] P.N. Batalha, L.S.M. Forezi, C.G.S. Lima, F.P. Pauli, F.C.S. Boechat, M.C.B.V. de Souza, A.C. Cunha, V.F. Ferreira, F.d.C. da Silva, Drug repurposing for the treatment of COVID-19: pharmacological aspects and synthetic approaches,

Bioorg. Chem. 106 (2021) 104488, https://doi.org/10.1016/j.bioorg.2020.104488.
[68] A.d.S. Antonio, L.S.M. Wiedemann, V.F. Veiga-Junior, Natural products' role against COVID-19, RSC Adv. 10 (39) (2020) 23379–23393, https://doi.org/10.1039/D0RA03774E.
[69] P. Gougis, C. Fenioux, C. Funck-Brentano, M. Veyri, J. Gligorov, C. Solas, J.-P. Spano, Anticancer drugs and COVID-19 antiviral treatments in patients with cancer: what can we safely use? Eur. J. Cancer 136 (2020) 1–3, https://doi.org/10.1016/j.ejca.2020.05.027.
[70] M. Aldea, J.-M. Michot, F.-X. Danlos, A. Ribas, J.-C. Soria, Repurposing of anticancer drugs expands possibilities for antiviral and anti-inflammatory discovery in COVID-19, Cancer Discov. 11 (6) (2021) 1336–1344, https://doi.org/10.1158/2159-8290.CD-21-0144.
[71] J. Wang, B. Liang, Y. Chen, J.F.-W. Chan, S. Yuan, H. Ye, L. Nie, J. Zhou, Y. Wu, M. Wu, L.S. Huang, J. An, A. Warshel, K.-Y. Yuen, A. Ciechanover, Z. Huang, Y. Xu, A new class of α-ketoamide derivatives with potent anticancer and anti-SARS-CoV-2 activities, Eur. J. Med. Chem. 215 (2021) 113267, https://doi.org/10.1016/j.ejmech.2021.113267.
[72] D. Díaz-Carballo, A.H. Acikelli, J. Klein, H. Jastrow, P. Dammann, T. Wyganowski, C. Guemues, S. Gustmann, W. Bardenheuer, S. Malak, N.S. Tefett, V. Khosrawipour, U. Giger-Pabst, A. Tannapfel, D. Strumberg, Therapeutic potential of antiviral drugs targeting chemorefractory colorectal adenocarcinoma cells overexpressing endogenous retroviral elements, J. Exp. Clin. Cancer Res. 34 (2015) 81, https://doi.org/10.1186/s13046-015-0199-5.
[73] A. Mostafa, A. Kandeil, Y.A.M.M. Elshaier, O. Kutkat, Y. Moatasim, A.A. Rashad, M. Shehata, M.R. Gomaa, N. Mahrous, S.H. Mahmoud, M. GabAllah, H. Abbas, A. El Taweel, A.E. Kayed, M.N. Kamel, M. El Sayes, D.B. Mahmoud, R. El-Shesheny, G. Kayali, M.A. Ali, FDA-approved drugs with potent in vitro antiviral activity against severe acute respiratory syndrome coronavirus 2, Pharmaceuticals 13 (2020) 443, https://doi.org/10.3390/ph13120443.
[74] Z. Chen, Y. Luo, A. Fang, C. Fan, C. Zeng, Synthesis of novel SN38-aspirin prodrugs for the treatment of hepatocellular carcinoma, Turk. J. Chem. 42 (2018) 929–939, https://doi.org/10.3906/kim-1801-21.
[75] V.U. Jeankumar, M. Chandran, G. Samala, M. Alvala, P.V. Koushik, P. Yogeeswari, E.G. Salina, D. Sriram, Development of 5-nitrothiazole derivatives: Identification of leads against both replicative and latent *Mycobacterium tuberculosis*, Bioorg. Med. Chem. Lett. 22 (2012) 7414–7417. dx.doi.org/10.1016/j.bmcl.2012.10.060.
[76] H. Sharma, S. Patil, T.W. Sanchez, N. Neamati, R.F. Schinazi, J.K. Buolamwini, Synthesis, biological evaluation and 3D-QSAR studies of 3-keto salicylic acid chalcones and related amides as novel HIV-1 integrase inhibitors, Bioorg. Med. Chem. 19 (6) (2011) 2030–2045, https://doi.org/10.1016/j.bmc.2011.01.047.
[77] J.R. Dimmock, M.P. Padmanilayam, R.N. Puthucode, A.J. Nazarali, N. L. Motaganahalli, G.A. Zello, J.W. Quail, E.O. Oloo, H.-B. Kraatz, J.S. Prisciak, T. M. Allen, C.L. Santos, J. Balzarini, E. De Clercq, E.K. Manavathu, A conformational and structure-activity relationship study of cytotoxic 3,5-bis (arylidene)-4-piperidones and related *N*-acryloyl analogues, J. Med. Chem. 44 (2001) 586–593, https://doi.org/10.1021/jm0002580.
[78] J. Wu, Y. Zhang, Y. Cai, J. Wang, B. Weng, Q. Tang, X. Chen, Z. Pan, G. Liang, S. Yang, Discovery and evaluation of piperid-4-one-containing mono-carbonyl analogs of curcumin as anti-inflammatory agents, Bioorg. Med. Chem. 21 (11) (2013) 3058–3065, https://doi.org/10.1016/j.bmc.2013.03.057.
[79] A.S. Girgis, S.S. Panda, A.M. Srour, A. Abdelnaser, S. Nasr, Y. Moatasim, O. Kutkat, A. El Taweel, A. Kandeil, A. Mostafa, M.A. Ali, N.G. Fawzy, M. S. Bekheit, E.M. Shalaby, L. Gigli, W. Fayad, A.A.F. Soliman, 3-Alkenyl-2-oxindoles: synthesis, antiproliferative and antiviral properties against SARS-CoV-2, Bioorg. Chem. 114 (2021) 105131, https://doi.org/10.1016/j.bioorg.2021.105131.
[80] https://www.cancer.gov/about-cancer/treatment/drugs/fluorouracil.
[81] https://www.cancer.gov/about-cancer/treatment/drugs/fluorouracil-topical.
[82] https://www.drugs.com/history/sutent.html.
[83] https://www.cancer.gov/about-cancer/treatment/drugs/sunitinibmalate.
[84] Carlo Riccardi, Ildo Nicoletti, Analysis of apoptosis by propidium iodide staining and flow cytometry, Nat. Protoc. 1 (3) (2006) 1458–1461, https://doi.org/10.1038/nprot.2006.238.
[85] I.A. Seliem, S.S. Panda, A.S. Girgis, Y. Moatasim, A. Kandeil, A. Mostafa, M.A. Ali, E.S. Nossier, F. Rasslan, A.M. Srour, R. Sakhuja, T.S. Ibrahim, Z.K.M. Abdel-samii, A.M.M. Al-Mahmoudy, New quinoline-triazole conjugates: synthesis, and antiviral properties against SARS-CoV-2, Bioorg. Chem. 114 (2021) 105117, https://doi.org/10.1016/j.bioorg.2021.105117.
[86] I.A. Seliem, A.S. Girgis, Y. Moatasim, A. Kandeil, A. Mostafa, M.A. Ali, M.S. Bekheit, S.S. Panda, New pyrazine conjugates: Synthesis, computational studies, and antiviral properties against SARS-CoV-2. ChemMedChem (in press). doi.org/10.1002/cmdc.202100476.
[87] Z. Schrank, G. Chhabra, L. Lin, T. Iderzorig, C. Osude, N. Khan, A. Kuckovic, S. Singh, R.J. Miller, N. Puri, Current molecular-targeted therapies in NSCLC and their mechanism of resistance, Cancers (Basel) 10 (2018) 224–241, https://doi.org/10.3390/cancers10070224.
[88] A. Ayati, S. Emami, S. Moghimi, A. Foroumadi, Thiazole in the targeted anticancer drug discovery, Future Med. Chem. 11 (15) (2019) 1929–1952, https://doi.org/10.4155/fmc-2018-0416.
[89] X. Liang, Q. Yang, P. Wu, C. He, L. Yin, F. Xu, Z. Yin, G. Yue, Y. Zou, L. Li, X. Song, C. Lv, W. Zhang, B. Jing, The synthesis review of the approved Tyrosine kinase inhibitors for anticancer therapy in 2015–2020, Bioorg. Chem. 113 (2021) 105011, https://doi.org/10.1016/j.bioorg.2021.105011.
[90] W. Zheng, Y. Zhao, Q. Luo, Y. Zhang, K. Wu, F.Y. Wang, Multi-targeted anticancer agents, Curr. Top. Med. Chem. 17 (2017) 3084–3098, https://doi.org/10.2174/1568026617666170707124126.
[91] R.-g. Fu, Y. Sun, W.-b. Sheng, D.-f. Liao, Designing multi-targeted agents: An emerging anticancer drug discovery paradigm, Eur. J. Med. Chem. 136 (2017) 195–211. dx.doi.org/10.1016/j.ejmech.2017.05.016.
[92] K. Kubo, T. Shimizu, S.-I. Ohyama, H. Murooka, A. Iwai, K. Nakamura, K. Hasegawa, Y. Kobayashi, N. Takahashi, K. Takahashi, S. Kato, T. Izawa, T. Isoe, Novel potent orally active selective VEGFR-2 tyrosine kinase inhibitors: synthesis, structure-activity relationships, and antitumor activities of *N*-Phenyl-*N*′-{4-(4-quinolyloxy)phenyl}ureas, J. Med. Chem. 48 (2005) 1359–1366, https://doi.org/10.1021/jm030427r.
[93] M. Shibuya, Vascular endothelial growth factor (VEGF) and its receptor (VEGFR) signaling in angiogenesis: a crucial target for anti- and pro-angiogenic therapies, Genes & Cancer 2 (2011) 1097–1105, https://doi.org/10.1177/1947601911423031.
[94] A.-K. Olsson, A. Dimberg, J. Kreuger, L. Claesson-Welsh, VEGF receptor signaling in control of vascular function, Nat. Rev. Mol. Cell Biol. 7 (2006) 359–371, https://doi.org/10.1038/nrm1911.
[95] Y. Zhang, Y. Chen, D. Zhang, L. Wang, T. Lu, Y. Jiao, Discovery of novel potent VEGFR-2 inhibitors exerting significant antiproliferative activity against cancer cell lines, J. Med. Chem. 61 (1) (2018) 140–157, https://doi.org/10.1021/acs.jmedchem.7b01091.
[96] C. Fontanella, E. Ongaro, S. Bolzonello, M. Guardascione, G. Fasola, G. Aprile, Clinical advances in the development of novel VEGFR2 inhibitors, Ann. Transl. Med. 2 (2014) 123–132, https://doi.org/10.3978/j.issn.2305-5839.2014.08.14.
[97] Santa Cruz Biotechnology, Inc., Oregon, USA, VEGFR2 (A-3): sc-6251 (www.scbt.com).
[98] K. Kyriakopoulou, E. Kefali, Z. Piperigkou, H. Bassiony, N.K. Karamanos, Advances in targeting epidermal growth factor receptor signaling pathway in mammary cancer, Cell. Signal. 51 (2018) 99–109, https://doi.org/10.1016/j.cellsig.2018.07.010.
[99] C.L. Arteaga, J.A. Engelman, ERBB receptors: from oncogene discovery to basic science to mechanism-based cancer therapeutics, Cancer Cell 25 (3) (2014) 282–303, https://doi.org/10.1016/j.ccr.2014.02.025.
[100] T. Yamaoka, M. Ohba, T. Ohmori, Molecular-targeted therapies for epidermal growth factor receptor and its resistance mechanisms, Inter. J. Mol. Sci. 18 (2017) 2420, https://doi.org/10.3390/ijms18112420.
[101] Santa Cruz Biotechnology, Inc., Oregon, USA, EGFR (528): sc-120 (www.scbt.com).
[102] L. Chen, H. Deng, H. Cui, J. Fang, Z. Zuo, J. Deng, Y. Li, X. Wang, L. Zhao, Inflammatory responses and inflammation-associated diseases in organs, Oncotarget 9 9 (6) (2018) 7204–7218, https://doi.org/10.18632/oncotarget.23208.
[103] S. Skeoch, I.N. Bruce, Atherosclerosis in rheumatoid arthritis: is it all about inflammation? Nat. Rev. Rheumatol. 11 (7) (2015) 390–400, https://doi.org/10.1038/nrrheum.2015.40.
[104] J.V. Fahy, Type 2 inflammation in asthmadpresent in most, absent in many, Nat. Rev. Immunol. 15 (2015) 57–65, https://doi.org/10.1038/nri3786.
[105] L.M. Coussens, Z. Werb, Inflammation and cancer, Nature 420 (6917) (2002) 860–867, https://doi.org/10.1038/nature01322.
[106] R. Medzhitov, Inflammation: new adventures of an old flame, Cell 140 (2010) (2010) 771–776, https://doi.org/10.1016/j.cell.2010.03.006.
[107] S.K. Shrivastava, P. Srivastava, R. Bandresh, P.N. Tripathi, A. Tripathi, Design, synthesis, and biological evaluation of some novel indolizine derivatives as dual cyclooxygenase and lipoxygenase inhibitor for anti-inflammatory activity, Bioorg. Med. Chem. 25 (16) (2017) 4424–4432, https://doi.org/10.1016/j.bmc.2017.06.027.
[108] D.L. Simmons, R.M. Botting, T. Hla, Cyclooxygenase isozymes: the biology of prostaglandin synthesis and inhibition, Pharmacol. Rev. 56 (2004) 387–437, https://doi.org/10.1124/pr.56.3.3.
[109] M.H. Yang, K.D. Yoon, Y.-W. Chin, J.H. Park, J. Kim, Phenolic compounds with radical scavenging and cyclooxygenase-2 (COX-2) inhibitory activities from *Dioscorea opposite*, Bioorg. Med. Chem. 17 (2009) 2689–2694, https://doi.org/10.1016/j.bmc.2009.02.057.
[110] D. Rambabu, N. Mulakayala, Ismail, K. Ravi Kumar, G. Pavan Kumar, C. Mulakayala, C.S. Kumar, A.M. Kalle, M.V. Basaveswara Rao, S. Oruganti, M. Pal, Synthesis and pharmacological evaluation of N-substituted 2-(2-oxo-2H-chromen-4-yloxy)propanamide as cyclooxygenase inhibitors, Bioorg. Med. Chem. Lett. 22 (21) (2012) 6745–6749, https://doi.org/10.1016/j.bmcl.2012.08.082.
[111] COX-1 Inhibitor Screening Kit (Fluorometric), Catalog#K548-100, BioVision Incorporated, CA 95035 USA, www.biovision.com.
[112] COX-2 Inhibitor Screening Kit (Fluorometric), Catalog#K547-100, BioVision Incorporated, CA 95035 USA, www.biovision.com.
[113] Discovery Studio 2.5, Accelrys Software Inc. (http://www.accelrys.com).
[114] https://www.rcsb.org/structure/4G5P.
[115] F. Solca, G. Dahl, A. Zoephel, G. Bader, M. Sanderson, C. Klein, O. Kraemer, F. Himmelsbach, E. Haaksma, G.R. Adolf, Target binding properties and cellular activity of Afatinib (BIBW 2992), an irreversible ErbB family blocker, J. Pharmacol. Exp. Ther. 343 (2) (2012) 342–350.
[116] https://www.drugs.com/history/gilotrif.html.
[117] https://www.cancer.gov/publications/dictionaries/cancer-drug/def/afatinib-dimaleate.